JOC Article

Synthesis and Electronic Properties of Regioisomerically Pure Oxochlorins

Masahiko Taniguchi,[†] Han-Je Kim,[†] Doyoung Ra,[†] Jennifer K. Schwartz,[‡] Christine Kirmaier,[‡] Eve Hindin,[‡] James R. Diers,[§] Sreedharan Prathapan,*[,†,||] David F. Bocian,*[,§] Dewey Holten,*[,‡] and Jonathan S. Lindsey*[,†]

Department of Chemistry, North Carolina State University, Raleigh, North Carolina 27695-8204, Department of Chemistry, Washington University, St. Louis, Missouri 63130-4899, and Department of Chemistry, University of California, Riverside, California 92521-0403

jlindsey@ncsu.edu

Received April 19, 2002

We describe a two-step conversion of C-alkylated zinc chlorins to zinc oxochlorins wherein the keto group is located in the reduced ring (17-position) of the macrocycle. The transformation proceeds by hydroxylation upon exposure to alumina followed by dehydrogenation with DDQ. The reactions are compatible with ethyne, iodo, ester, trimethylsilyl, and pentafluorophenyl groups. A route to a spirohexyl-substituted chlorin/oxochlorin has also been developed. Representative chlorins and oxochlorins were characterized by static and time-resolved absorption spectroscopy and fluorescence spectroscopy, resonance Raman spectroscopy, and electrochemistry. The fluorescence quantum yields of the zinc oxochlorins ($\Phi_f = 0.030-0.047$) or free base (Fb) oxochlorins ($\Phi_f = 0.13-0.16$) are comparable to those of zinc tetraphenylporphyrin (ZnTPP) or free base tetraphenylporphyrin (FbTPP), respectively. The excited-state lifetimes of the zinc oxochlorins ($\tau = 0.5-0.7$ ns) are on average 4-fold lower than that of ZnTPP, and the lifetimes of the Fb oxochlorins ($\tau = 7.4-8.9$ ns) are ~40% shorter than that of FbTPP. Time-resolved absorption spectroscopy of a zinc oxochlorin indicates the yield of intersystem crossing is >70%. Resonance Raman spectroscopy of copper oxochlorins show strong resonance enhancement of the keto group upon Soret excitation but not with Q_y-band excitation, which is attributed to the location of the keto group in the reduced ring (rather than in the isocyclic ring as occurs in chlorophylls). The one-electron oxidation potential of the zinc oxochlorins is shifted to more positive potentials by approximately 240 mV compared with that of the zinc chlorin. Collectively, the fluorescence yields, excited-state lifetimes, oxidation potentials, and various spectral characteristics of the chlorin and oxochlorin building blocks provide the foundation for studies of photochemical processes in larger architectures based on these chromophores.

Introduction

Synthetic building blocks that exhibit the spectral and photochemical properties of chlorophyll would have wide application in bioorganic and materials chemistry, particularly in areas such as photodynamic therapy, light-harvesting model systems, and molecular photonics. In many instances where chlorophyll-like molecules are desired, porphyrins have been employed as surrogates. Porphyrins and chlorophyll differ in two key structural elements (Chart 1): (1) Chlorophyll is a dihydroporphyrin in which one of the β-pyrrole bonds is saturated (commonly designated a chlorin). (2) Chlorophyll contains an exocyclic ring bearing a keto group that is conjugated with the π-electron system of the macrocycle. These structural differences between porphyrins and chlorins (chlorophylls) have significant effects both on the synthetic methods that can be employed to construct the basic ring system and on the physical, electronic, and spectral properties of the macrocycle. As a consequence, the use of porphyrin surrogates typically involves trade offs in either synthetic or physicochemical properties.

Porphyrins are generally superior to chlorins from the standpoint of synthetic malleability and chemical stability. In particular, the absence of a saturated β-pyrrole bond makes porphyrins much less susceptible to oxidative damage. These features of porphyrins have permitted the preparation of a large variety of chemically robust building blocks bearing peripheral substituents that provide synthetic handles, impart desired solubility, and tune redox potentials. On the other hand, chlorins are superior to porphyrins for use in photosynthetic systems and related photochemical systems wherein broad spectral coverage and/or efficient through-space contributions to energy transfer are desired. This superiority arises because (1) the extinction coefficient of the long-wavelength absorption band of chlorins is greater than that of porphyrins,[1] affording strong absorption in the near-

[†] North Carolina State University.
[‡] Washington University.
[§] University of California.
[||] Permanent address: Department of Applied Chemistry, Cochin University of Science and Technology, Cochin, India 682022.

10.1021/jo025843i CCC: $22.00
Published on Web 09/24/2002

CHART 1

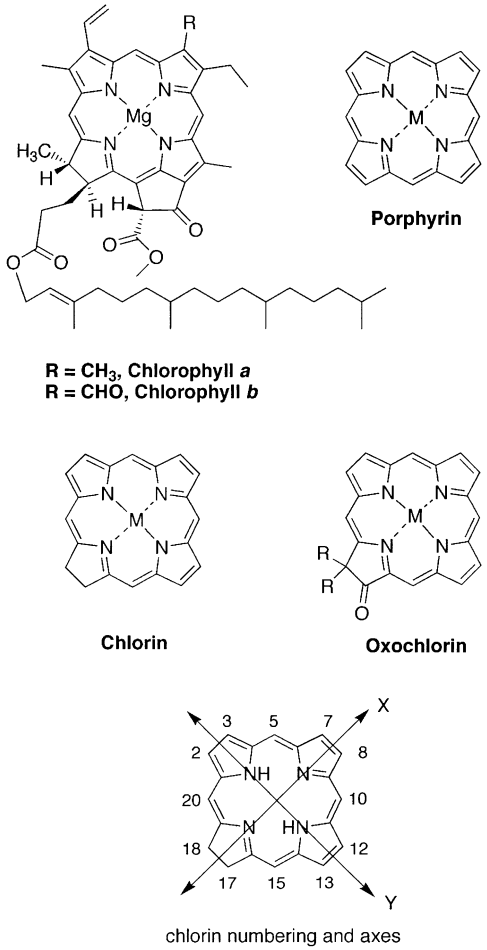

IR region; and (2) chlorins are linear oscillators whereas metalloporphyrins are planar oscillators,[2] enabling greater directionality in intermolecular energy transfer in the former versus the latter.

The important photochemical properties of chlorins have motivated the development of a number of new syntheses of these green pigments in the past few years.[3−12] Earlier syntheses have been reviewed.[13] We recently developed a rational synthesis of C-methylated chlorin building blocks.[3,8,9] Each chlorin bears one geminal dimethyl group at the β-position in the reduced ring. For building block applications, we have introduced synthetic handles at several β-positions (2, 8, 12) and two meso-positions (5, 10). One of our objectives is to create arrays containing a large number of chlorin chromophores, thereby obtaining synthetic materials with features that more closely resemble the natural light-harvesting systems. The utilization of chlorin building blocks in multipigment arrays requires the ability to manipulate the fundamental photophysical and electronic properties of the chlorin chromophore, as is now routinely done with porphyrins.

One type of modified chlorin that is frequently encountered is an oxochlorin, wherein a keto group is present at one of the β-carbons in the reduced ring (Chart 1). The motivation for forming an oxochlorin has typically stemmed from synthetic considerations: treatment of a β,β'-disubstituted porphyrin with an oxidizing agent such as hydrogen peroxide[14−17] or OsO_4[18−21] followed by acid-catalyzed pinacol rearrangement of the resulting diol[14−21] yields the oxochlorin. In this manner, readily available synthetic porphyrins serve as starting materials for preparing chlorin derivatives.[22] Though widely applied with β-alkylated porphyrins, this approach has two critical limitations: (1) Application to a β-unsubstituted porphyrin would result in keto−enol tautomerism, thereby causing reversion of the oxochlorin to the hydroxyporphyrin.[20] (2) Multiple oxochlorin isomers typically result with porphyrins wherein the four pyrrole rings bear nonidentical substituents,[17−19,23,24] different substituents (e.g., methyl/ethyl) are present at the two β-positions of the pyrrole ring that is attacked by OsO_4,[17−19] or the presence of meso-substituents causes the symmetry of the porphyrin to be less than 4-fold.[24−27]

In this paper, we report an efficient method for converting C-alkylated chlorins to the corresponding

(1) Smith, J. H. C.; Benitez, A. In *Modern Methods of Plant Analysis*; Paech, K., Tracey, M. V., Eds.; Springer-Verlag: Berlin, 1955; Vol. IV, pp 142−196.
(2) (a) Gurinovich, G. P.; Sevchenko, A. N.; Solov'ev, K. N. *Opt. Spectrosc.* **1961**, *10*, 396−401. (b) Gouterman, M.; Stryer, L. *J. Chem. Phys.* **1962**, *37*, 2260−2266.
(3) Taniguchi, M.; Ra, D.; Mo, G.; Balasubramanian, T.; Lindsey, J. S. *J. Org. Chem.* **2001**, *66*, 7342−7354.
(4) Jacobi, P. A.; Lanz, S.; Ghosh, I.; Leung, S. H.; Löwer, F.; Pippin, D. *Org. Lett.* **2001**, *3*, 831−834.
(5) Montforts, F.-P.; Kutzki, O. *Angew. Chem., Int. Ed.* **2000**, *39*, 599−601.
(6) Shea, K. M.; Jaquinod, L.; Khoury, R. G.; Smith, K. M. *Tetrahedron* **2000**, *56*, 3139−3144.
(7) Burns, D. H.; Shi, D. C.; Lash, T. D. *Chem. Commun.* **2000**, 299−300.
(8) (a) Strachan, J.-P.; O'Shea, D. F.; Balasubramanian, T.; Lindsey, J. S. *J. Org. Chem.* **2000**, *65*, 3160−3172. (b) Strachan, J.-P.; O'Shea, D. F.; Balasubramanian, T.; Lindsey, J. S. *J. Org. Chem.* **2001**, *66*, 642.
(9) Balasubramanian, T.; Strachan, J. P.; Boyle, P. D.; Lindsey, J. S. *J. Org. Chem.* **2000**, *65*, 7919−7929.
(10) Krattinger, B.; Callot, H. J. *Eur. J. Org. Chem.* **1999**, 1857−1867.
(11) Johnson, C. K.; Dolphin, D. *Tetrahedron Lett.* **1998**, *39*, 4619−4622.
(12) Mironov, A. F.; Efremov, A. V.; Efremova, O. A.; Bonnett, R.; Martinez, G. *J. Chem. Soc., Perkin Trans. 1* **1998**, 3601−3608.
(13) (a) Montforts, F.-P.; Gerlach, B.; Höper, F. *Chem. Rev.* **1994**, *94*, 327−347. (b) Flitsch, W. *Adv. Heterocycl. Chem.* **1988**, *43*, 73−126. (c) Montforts, F.-P.; Glasenapp-Breiling, M. *Prog. Heterocycl. Chem.* **1998**, *10*, 1−24.
(14) Bonnett, R.; Dolphin, D.; Johnson, A. W.; Oldfield, D.; Stephenson, G. F. *Proc. Chem. Soc. London* **1964**, 371−372.
(15) Bonnett, R.; Dimsdale, M. J.; Stephenson, G. F. *J. Chem. Soc. C* **1969**, 564−570.
(16) Chang, C. K. *Biochemistry* **1980**, *19*, 1971−1976.
(17) Chang, C. K.; Wu, W. *J. Org. Chem.* **1986**, *51*, 2134−2137.
(18) Chang, C. K.; Sotiriou, C. *J. Org. Chem.* **1985**, *50*, 4989−4991.
(19) Chang, C. K.; Sotiriou, C. *J. Heterocycl. Chem.* **1985**, *22*, 1739−1741.
(20) Brückner, C.; Dolphin, D. *Tetrahedron Lett.* **1995**, *36*, 3295−3298.
(21) Inhoffen, H. H.; Nolte, W. *Liebigs Ann. Chem.* **1969**, *725*, 167−176.
(22) For a method for converting heme into an oxochlorin, see: Bats, J. W.; Haake, G.; Meier, A.; Montforts, F.-P.; Scheurich, G. *Liebigs Ann.* **1995**, 1617−1631.
(23) Sotiriou, C.; Chang, C. K. *J. Am. Chem. Soc.* **1988**, *110*, 2264−2270.
(24) Chen, Y.; Medforth, C. J.; Smith, K. M.; Alderfer, J.; Dougherty, T. J.; Pandey, R. K. *J. Org. Chem.* **2001**, *66*, 3930−3939.
(25) Osuka, A.; Marumo, S.; Maruyama, K. *Bull. Chem. Soc. Jpn.* **1993**, *66*, 3837−3839.
(26) Osuka, A.; Marumo, S.; Maruyama, K.; Mataga, N.; Tanaka, Y.; Taniguchi, S.; Okada, T.; Yamazaki, I.; Nishimura, Y. *Bull. Chem. Soc. Jpn.* **1995**, *68*, 262−276.
(27) Osuka, A.; Marumo, S.; Mataga, N.; Taniguchi, S.; Okada, T.; Yamazaki, I.; Nishimura, Y.; Ohno, T.; Nozaki, K. *J. Am. Chem. Soc.* **1996**, *118*, 155−168.

oxochlorins. Our motivation for preparing oxochlorins stems not as a means of converting porphyrins to chlorins but from the greater redox stability of oxochlorins compared with chlorins.[25,28−30] The keto group is introduced at the site (17-position) adjacent to the geminal dialkyl group (18-position), forming only one oxochlorin isomer regardless of the substitution pattern at the perimeter of the macrocycle. The method has been applied to chlorins bearing a variety of substituents, including chlorins with a spiroalkyl unit in place of the geminal dimethyl unit in the reduced ring. Oxochlorins in various metalation states (Zn, Mg, Cu, free base (Fb)) also have been prepared. The metallo and Fb oxochlorins have been characterized by electrochemistry, static and time-resolved absorption and fluorescence spectroscopy, and resonance Raman spectroscopy.

Results and Discussion

A. Synthesis. 1. Method for Forming Oxochlorins. Reagents for the oxidation of a benzylic methylene unit to the corresponding carbonyl or hydroxy group are well-known, including MnO_2, $Cu(OAc)_2$, SeO_2, and CrO_3. However, treatment of **Zn1**[8] with MnO_2, $Cu(OAc)_2$, or SeO_2 proved ineffective, while CrO_3 led to extensive decomposition. Given the facile hydroxylation of certain chlorins during chromatography on neutral alumina,[31] and in some cases the direct formation of oxochlorins (albeit in low yield),[32] we decided to explore this "side-reaction" as the first step in a procedure for converting chlorins to oxochlorins. Thus, treatment of a mixture of **Zn1** and basic alumina (activity I) in toluene at 60 °C exposed to air for 22 h resulted in three components identified by TLC and laser desorption mass spectrometry (LD-MS) analysis as unchanged starting material (**Zn1**, 2%), oxochlorin (**Oxo-Zn1**, 23%), and hydroxychlorin (**HO-Zn1**, 52%) (Scheme 1). The three components were easily separated by column chromatography on silica.

During the development of this method, a number of factors that affect the course of hydroxylation were identified. (1) The reaction proceeded well in toluene but not in dichloromethane. (2) The reaction was more efficient with basic alumina (activity I) than with neutral alumina or basic alumina (activity V). (3) The reaction at 50−60 °C required 4−20 h whereas up to 60 h was required at room temperature. (4) Attempts to use the Fb chlorin or the Cu chlorin led to recovery of starting material.

The conversion of the hydroxychlorin **HO-Zn1** to the corresponding oxochlorin was examined. After surveying several reagents (SeO_2, *p*-chloranil, MnO_2), we turned to the use of DDQ. The oxidation of **HO-Zn1** with ∼2 equiv of DDQ in toluene proceeded rapidly and gave **Oxo-Zn1** in 47% yield.

SCHEME 1

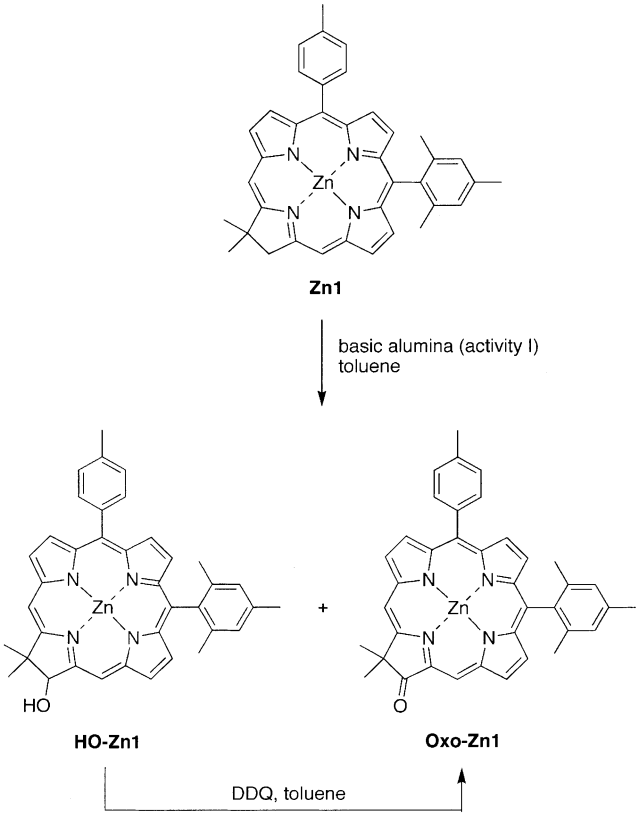

The success of these two reactions prompted the development of a two-step process without purification of the intermediate hydroxychlorin. Thus, treatment of **Zn1** with alumina (activity I) in toluene at 50 °C for 6.5 h, filtration to remove the alumina, and treatment of the crude product from the filtrate with DDQ in toluene for 5 min gave **Oxo-Zn1** in 53% yield. This procedure provides a simple means of transforming the chlorin to the corresponding oxochlorin.

The scope of the method was evaluated by the application to chlorins bearing a variety of peripheral functional groups. The functional groups include strong electron-withdrawing groups (**Zn2**), groups for surface attachment following deprotection (**Zn3**), and groups for the Pd-mediated synthesis of multi-chlorin arrays (**Zn4**, **Zn5**).[3] Zn chlorins **Zn2**−**Zn5** were readily converted into Zn oxochlorins **Oxo-Zn2**−**Oxo-Zn5** via the two-step alumina/DDQ procedure described above (Scheme 2). This method is complementary to the CrO_3−dimethylpyrazole oxidation employed in the synthesis of the dioxobacteriochlorin compound tolyporphin.[33]

2. Spiro-Chlorins/Oxochlorins. A typical design of porphyrin building blocks employs several peripheral sites for attachment of synthetic handles and others for positioning of groups that impart high solubility in organic solvents. Methodology has been developed for introducing four different groups of wide variety at the four meso-positions of porphyrins.[34] In the case of chlorins, methodology exists for introducing two meso-sub-

(28) Chang, C. K.; Barkigia, K. M.; Hanson, L. K.; Fajer, J. *J. Am. Chem. Soc.* **1986**, *108*, 1352−1354.
(29) Stolzenberg, A. M.; Glazer, P. A.; Foxman, B. M. *Inorg. Chem.* **1986**, *25*, 983−991.
(30) Zaleski, J. M.; Chang, C. K.; Nocera, D. G. *J. Phys. Chem.* **1993**, *97*, 13206−13215.
(31) Burns, D. H.; Li, Y. H.; Shi, D. C.; Delaney, M. O. *Chem. Commun.* **1998**, 1677−1678.
(32) Battersby, A. R.; Fookes, C. J. R.; Snow, R. J. *J. Chem. Soc., Perkin Trans. 1* **1984**, 2725−2732.
(33) (a) Minehan, T. G.; Kishi, Y. *Tetrahedron Lett.* **1997**, *38*, 6811−6814. (b) Wang, W.; Kishi, Y. *Org. Lett.* **1999**, *1*, 1129−1132.
(34) Rao, P. D.; Dhanalekshmi, S.; Littler, B. J.; Lindsey, J. S. *J. Org. Chem.* **2000**, *65*, 7323−7344.

SCHEME 2

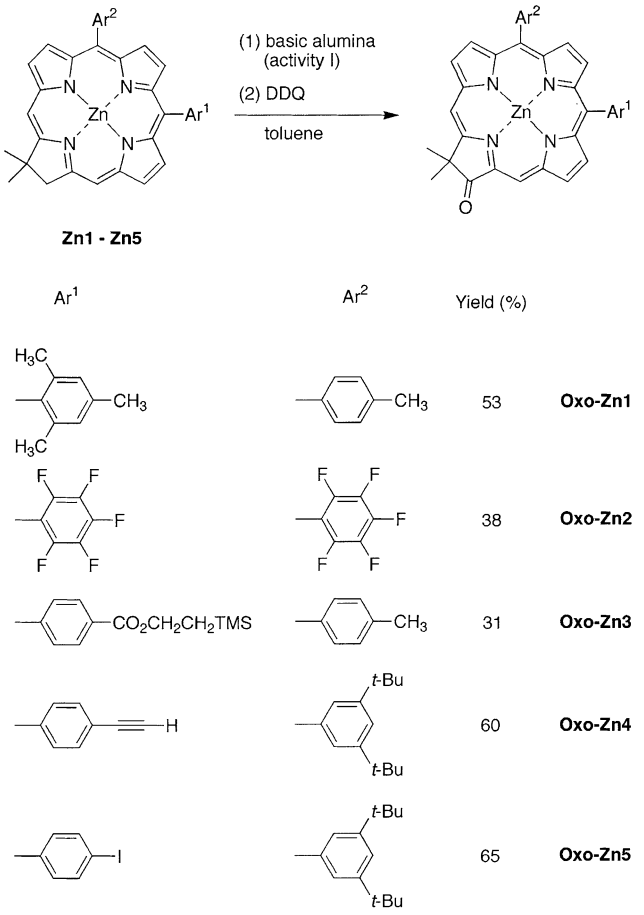

stituents, two β-substituents and one meso-substituent, or two meso-substituents and one β-substituent, but not for introducing more than three different groups.[3,8] The chief limitation is that the two meso-sites flanking the reduced ring are not yet accessible toward modification. To broaden the range of synthetic control over substituents at the perimeter of the chlorin macrocycle, we sought to investigate whether the site of the geminal dialkyl group (18-position) could serve as a position for introducing substituents. We investigated the synthesis of a chlorin bearing a spirohexyl group in lieu of a geminal dimethyl group (Scheme 3). Spirochlorins have been made previously as a means of converting a porphyrin to a chlorin[35] or as a side product from the intramolecular cyclization of a linker joining two chlorins in a photosynthetic model system.[36]

The synthesis of C-alkylated chlorins entails the joining of an Eastern half and a Western half.[3,8,9] The synthesis of a spirohexyl-substituted Western half begins in the same manner as for the *gem*-dimethyl-substituted Western half, with the conversion of pyrrole-2-carboxaldehyde to the nitroethyl pyrrole **6**. The prior synthesis of pyrrole **6**[8] required two steps and a tedious workup procedure. A simplified two-step, one-flask synthesis was developed that avoids isolation of the intermediate nitrovinyl pyrrole. In this manner, **6** was obtained in 66% yield compared with 45% in the prior procedure.

A key step in the synthesis of the desired spirohexyl Western half is the Michael addition of nitroethyl pyrrole **6** to an α,β-unsaturated ketone bearing a spirohexyl group at the β-positions. Cyclohexanone reacted smoothly with dimethyl (2-oxopropyl)phosphonate via a Wittig–Horner reaction[37] to yield the α,β-unsaturated ketone **7**.[38] Reaction of **7** with nitroethyl pyrrole **6** in the presence of CsF gave the Michael addition product **8**, from which tetrahydrodipyrrin *N*-oxide **9** was obtained following a straightforward procedure.[3] The latter was deoxygenated to form the tetrahydrodipyrrin Western half **10**.

The reaction of Western half **6** and Eastern half **11-OH**[8] under the standard two-step chlorin-forming conditions[3] gave the chlorin **Zn12** in 19% yield. Oxidation of **Zn12** under the conditions described above (alumina/DDQ) led to the corresponding oxochlorin **Oxo-Zn12**, albeit in only 20% yield (Scheme 3).

3. Free Base, Copper, and Magnesium Oxochlorins. The Fb chlorins **1**–**5** and oxochlorins **Oxo-1**–**Oxo-5** were obtained by demetalation of the corresponding Zn chelates with TFA in CH_2Cl_2 (Scheme 4). For resonance Raman studies, the Cu chelates of several chlorins and oxochlorins were prepared by treating the Fb species with $Cu(OAc)_2$ in CH_2Cl_2/methanol (1:1) at room temperature. Treatment of Fb oxochlorin **Oxo-1** or **Oxo-2** to the heterogeneous magnesium insertion procedure (MgI_2, DIEA, CH_2Cl_2)[39] at room temperature afforded the corresponding Mg chelate **Oxo-Mg1** or **Oxo-Mg2**. However, attempts to metalate **1** to give the Mg chlorin **Mg1** were unsuccessful as demetalation occurred upon workup.

4. Chemical Characterization. The chlorins and oxochlorins generally were characterized by absorption spectroscopy, fluorescence emission spectroscopy, LD-MS and/or high-resolution mass spectrometry, and ^{1}H NMR spectroscopy. The ^{1}H NMR spectra of the oxochlorins were generally unremarkable. As with the corresponding chlorins, each of the six β-protons and two meso-protons is unique and gives a distinctive resonance(s). In the metallo or free base oxochlorins, the resonances due to the protons at the 15 and 20 positions are shifted downfield by ~0.9 and 0.4 ppm, respectively, compared with those of the corresponding chlorins. Downfield shifts albeit of lesser magnitude also were observed for the peaks stemming from the meso-protons. One hallmark distinguishing the free base oxochlorins and chlorins stems from the resonances of the central NH protons. In both the free base chlorins and oxochlorins, the NH protons are not equivalent. However, the free base chlorins tend to give a single broad peak while the free base oxochlorins studied herein give two distinct peaks ($\Delta\delta$ ~0.15 ppm) at ~0.4 ppm higher field.

B. Physical Properties. 1. Absorption Spectra. Representative UV/vis absorption spectra of the chlorins

(35) (a) Collier, G. L.; Jackson, A. H.; Kenner, G. W. *J. Chem. Soc. C* **1967**, 66–72. (b) Smith, K. M.; Baptista de Almeida, J. A. P.; Lewis, W. M. *J. Heterocycl. Chem.* **1980**, *17*, 481–487. (c) Kai, S.; Suzuki, M. *Tetrahedron Lett.* **1996**, *37*, 5931–5934.

(36) (a) Zheng, G.; Alderfer, J. L.; Senge, M. O.; Shibata, M.; Dougherty, T. J.; Pandey, R. K. *J. Org. Chem.* **1998**, *63*, 6434–6435. (b) Zheng, G.; Shibata, M.; Dougherty, T. J.; Pandey, R. K. *J. Org. Chem.* **2000**, *65*, 543–557.

(37) Corey, E. J.; Smith, J. G. *J. Am. Chem. Soc.* **1979**, *101*, 1038–1039.

(38) Fukuda, Y.; Utimoto, K. *Bull. Chem. Soc. Jpn.* **1991**, *64*, 2013–2015.

(39) Lindsey, J. S.; Woodford, J. N. *Inorg. Chem.* **1995**, *34*, 1063–1069.

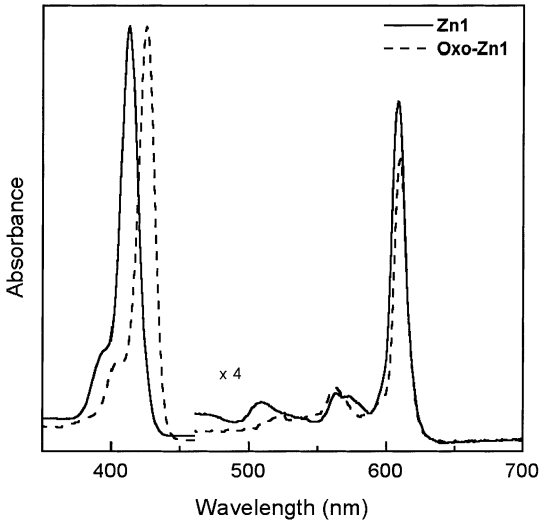

FIGURE 1. Absorption spectra of chlorin **Zn1** and oxochlorin **Oxo-Zn1** in toluene at room temperature.

and oxochlorins in toluene at room temperature are shown in Figures 1 and 2. For each compound, the position of the long-wavelength absorption band is listed in Table 1. The wavelength maxima of all the prominent features along with extinction coefficients are given in the Experimental Section.

The major absorption features of the chlorins and oxochlorins, and general differences between the two types of chromophore, are illustrated for **Oxo-Zn1** and **Zn1** in Figure 1. The strong near-UV Soret (B) band of the oxochlorin is red shifted by ~10 nm from its chlorin counterpart, while the $Q_y(0,0)$ band is relatively unchanged (609 versus 608 nm). Both bands are slightly sharper for the oxochlorin. Between these two major features for both compounds are the weaker Q_y vibronic transitions such as $Q_y(1,0)$ at ~575 nm and the corresponding Q_x bands in the green spectral region. The same spectral features are observed for the other Zn chlorin/oxochlorins, including **Zn4** and **Oxo-Zn4** (Figure 2B,D and Table 1).

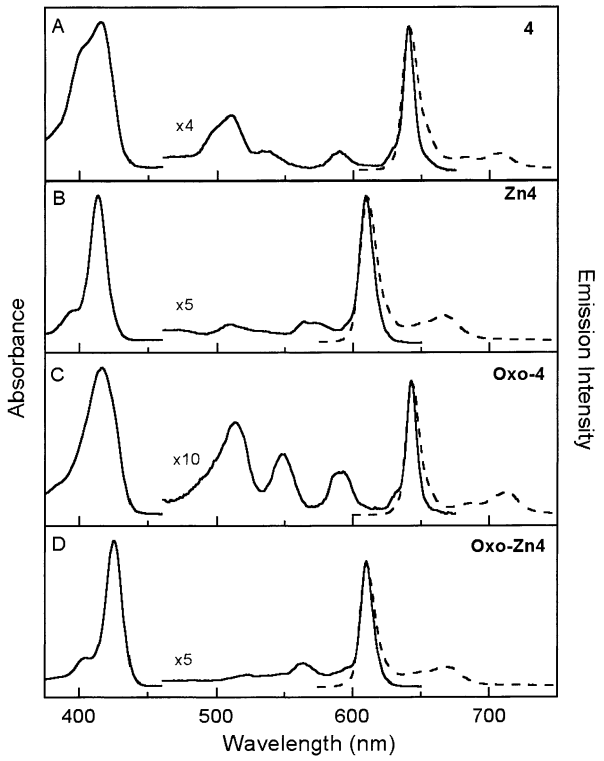

FIGURE 2. Absorption spectra (solid) and fluorescence spectra (dashed) of chlorins **4** (A) and **Zn4** (B) and oxochlorins **Oxo-4** (C) and **Oxo-Zn4** (D) in toluene at room temperature. The emission was elicited by excitation in the Soret region.

The spectra of Fb chlorins and oxochlorins are generally similar to those for the Zn-containing species, with several differences. (1) The long-wavelength absorption feature, the $Q_y(0,0)$ band, of each Fb compound is at ~640 nm, which is ~30 nm to the red of the corresponding Zn chelate (Table 1). This difference can be seen for **4** versus **Zn4** (Figure 2A,B) and for **Oxo-4** versus **Oxo-Zn4** (Figure 2C,D). (2) The near-UV Soret absorption of each Fb chromophore is much broader and is split into at least two features. The breadth and splitting in the Soret

SCHEME 3

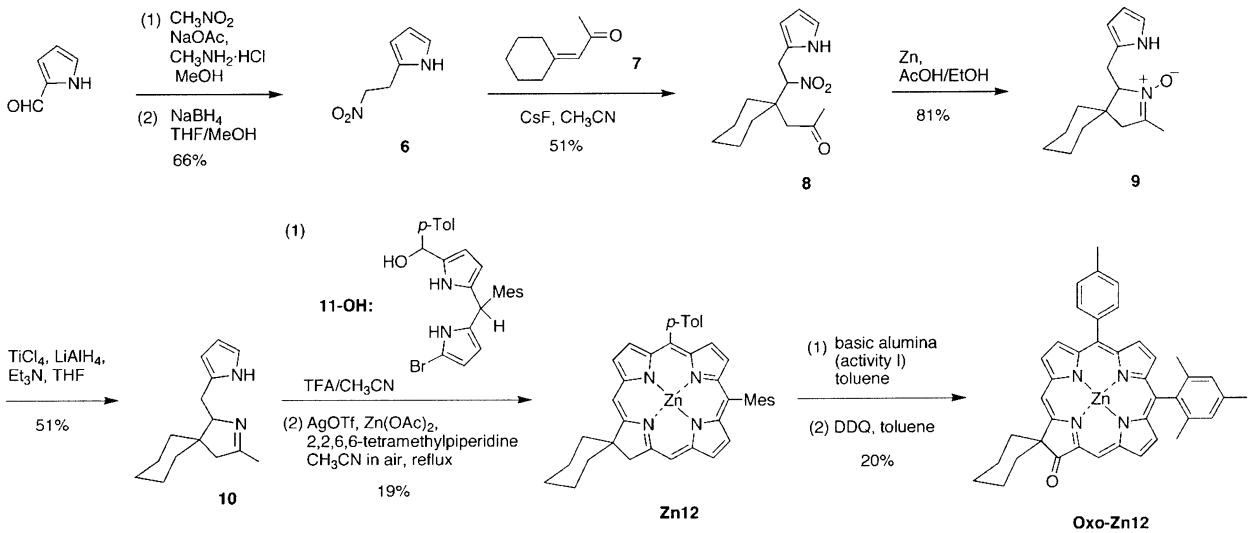

SCHEME 4

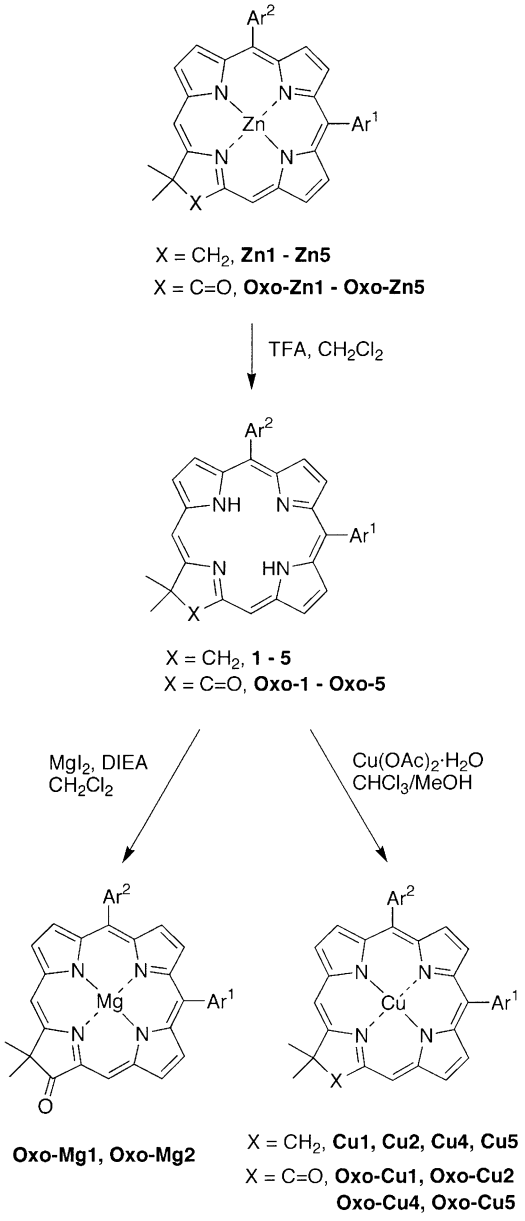

region is particularly noteworthy for the Fb chlorins such as **4** (Figure 2A), but is also present for the oxochlorin analogues such as **Oxo-4** (Figure 2C). (3) The general contour and amplitude ratios of the Q_x features in the 500−600 nm region are different for the Fb versus Zn complexes, including increased extinction coefficients for the Q_x features in the vicinity of 515 and 550 nm.

Some of the above characteristics are similar to those of the porphyrin analogues, including the red shift of the long-wavelength absorption band in Fb versus Zn complexes. However, for the chlorins and oxochlorins, this long-wavelength feature is the $Q_y(0,0)$ band, whereas it is the $Q_x(0,0)$ band in Fb porphyrins and the combined (degenerate) $Q_x(0,0)$ and $Q_y(0,0)$ band for the Zn porphyrins. Additionally, the extinction coefficient of the long-wavelength feature is on the average about 5-fold larger for the chlorin/oxochlorin. The splitting of the Soret band of the Fb versions of the latter macrocycles is also a prominent difference from the porphyrin counterparts. These characteristics ultimately derive from the presence of the reduced ring in the chlorins/oxochlorins, and to a much lesser degree to the asymmetric peripheral substituent patterns examined herein. These structural/electronic factors lower the symmetry compared to porphyrins, eliminate degeneracies associated with excited states and transitions, and influence the nature, energies and electron-density distributions of the frontier molecular orbitals. These issues have been discussed previously in comparing the electronic spectra of chlorins and porphyrins.[40]

2. Fluorescence Properties. Fluorescence spectra of the chlorins **4** and **Zn4** and the oxochlorin analogues **Oxo-4** and **Oxo-Zn4** are shown in Figure 2 (dashed). The wavelength of the $Q_y(0,0)$ emission maximum for each of these compounds and the other chlorins and oxochlorins are given in Table 1 along with the emission yields and fluorescence lifetimes. The emission wavelengths including the Q(0,1) position are given in the Experimental section.

The fluorescence spectra of all the chlorins and oxochlorins are dominated by a $Q_y(0,0)$ band and a weaker $Q_y(0,1)$ feature to longer wavelengths. One of the most notable characteristics of these emission spectra is the minimal "Stokes" shift between the $Q_y(0,0)$ absorption and emission maxima. This shift is well within 3 nm (<75 cm^{-1}) for all the chlorins and is typically within 1 nm (<25 cm^{-1}) for the oxochlorins. These absorption−fluorescence spacings are typically smaller than those of porphyrin analogues such as Zn(II)-*meso*-tetraphenylporphyrin (**ZnTPP**), *meso*-tetraphenylporphyrin (**FbTPP**), and β-octaethylporphyrins **ZnOEP** and **FbOEP**.[40,41] The especially small shifts for the oxochlorins must reflect particularly close similarity of the equilibrium structure in the ground and lowest excited singlet electronic states and, likely, only modest differences in the overall distribution of electron density.

The fluorescence quantum yield (Φ_f) of each Zn oxochlorin **Oxo-Zn1** - **Oxo-Zn4** is in the range of 0.030−0.047, which is similar to the value of 0.033[40] for **ZnTPP**. Each Fb oxochlorin **Oxo-1**−**Oxo-4** has a Φ_f value in the range of 0.13−0.16, which is comparable to the yield of 0.11[42] for **FbTPP**. The Φ_f for Mg oxochlorin **Oxo-Mg1** of 0.10 is slightly lower than the value of 0.16[40,43,44] for **MgTPP** and related compounds. In general, each oxochlorin examined has a Φ_f value that is approximately one-half to one-third that of the corresponding chlorin (Table 1). The values are generally in good agreement with the results of the measurements on the emission properties of chlorins and oxochlorins reported previously.[40,45−47]

(40) Gouterman, M. In *The Porphyrins*; Dolphin, D., Ed.; Academic Press: New York, 1978; Vol. III, pp 1−165.
(41) Retsek, J. L.; Medforth, C. J.; Nurco, D. J.; Gentemann, S., Chirvony, V. S.; Smith, K. M.; Holten, D. *J. Phys. Chem. B* **2001**, *105*, 6396−6411.
(42) Seybold, P. G.; Gouterman, M. *J. Mol. Spectrosc.* **1969**, *31*, 1−13.
(43) Yang, S. I.; Seth, J.; Strachan, J.-P.; Gentemann, S.; Kim, D.; Holten, D.; Lindsey, J. S.; Bocian, D. F. *J. Porphyrins Phthalocyanines* **1999**, *3*, 117−147.
(44) (a) Gradyushko, A. T.; Tsvirko, M. P. *Opt. Spectrosc.* **1971**, *31*, 291−295. (b) Harriman, A. *J. Chem. Soc., Faraday Trans. 2* **1981**, *77*, 1281−1291. (c) Politis, T. G.; Drickamer, H. G. *J. Chem. Phys.* **1982**, *76*, 285−291. (d) Ohno, O.; Kaizu, Y.; Kobayashi, H. *J. Chem. Phys.* **1985**, *82*, 1779−1787.

TABLE 1. Physical Properties of Chlorins and Oxochlorins[a]

compd	Ar[1] (10-position)	Ar[2] (5-position)	λ_{ab}[b] (nm)	λ_{em}[c] (nm)	Φ_f[d]	τ[e] (ns)	$(k_{rad})^{-1}$[f] (ns)	$E_{1/2}$[g] (V)
1	mesityl	*p*-tolyl	641	641	0.26[h]	9.2	35	
2	C_6F_5	C_6F_5	645	646	0.25[h]	7.3	29	
3	Ar[i]	*p*-tolyl	640	641	0.28	9.6	33	
4	4-ethynylphenyl	3,5-di-*t*-Bu-phenyl	641	642	0.30	9.6	31	
Zn1	mesityl	*p*-tolyl	608	609	0.083[h]	1.4	17	0.35
Zn2	C_6F_5	C_6F_5	616	619	0.087[h]	1.0	11	0.55
Zn3	Ar[i]	*p*-tolyl	609	611	0.095	1.5	16	
Zn4	4-ethynylphenyl	3,5-di-*t*-Bu-phenyl	609	612	0.085	1.4	12	
Zn12	mesityl	*p*-tolyl	610	611	0.15	1.3	4	
Oxo-1	mesityl	*p*-tolyl	643	643	0.13	8.9	68	
Oxo-2	C_6F_5	C_6F_5	645	645	0.15	7.4	49	
Oxo-3	Ar[i]	*p*-tolyl	643	643	0.16	8.8	55	
Oxo-4	4-ethynylphenyl	3,5-di-*t*-Bu-phenyl	643	643	0.14	8.8	63	
Oxo-Zn1	mesityl	*p*-tolyl	609	609	0.040	0.9	22	0.59
Oxo-Zn2	C_6F_5	C_6F_5	614	615	0.030	0.6	20	0.78
Oxo-Zn3	Ar[i]	*p*-tolyl	610	611	0.047	0.6	12	
Oxo-Zn4	4-ethynylphenyl	3,5-di-*t*-Bu-phenyl	610	612	0.044	0.7[j]	16	
Oxo-Zn12	mesityl	*p*-tolyl	611	612	0.04	0.7	18	
Oxo-Mg1	mesityl	*p*-tolyl	617	617	0.10	3.0	30	0.41
Oxo-Mg2	C_6F_5	C_6F_5	620	621	0.13	2.6	20	0.65

[a] Spectral measurements were performed in toluene at room temperature unless noted otherwise. [b] Position of the long-wavelength, $Q_y(0,0)$ absorption band rounded to the nearest nanometer. [c] Position of the $Q_y(0,0)$ emission band rounded to the nearest nanometer. [d] Fluorescence yield (±10%). [e] Excited-state lifetime determined for deoxygenated samples by fluorescence-modulation spectroscopy unless noted otherwise; the error is ±10% except for **OxoZn1**-**OxoZn4** where the error is ±0.1 ns. [f] Inverse of the radiative rate constant calculated from the fluorescence yield and excited-state lifetime data in the previous two columns using the relationship $(k_{rad})^{-1} = \tau/\Phi_f$. [g] $E_{1/2}$ vs Ag/Ag^+ in CH_2Cl_2 containing 0.1 M Bu_4NPF_6; $E_{1/2}$ of $FeCp_2/FeCp_2^+$ is 0.19 V. [h] Revised from the following values in ref 8: **1** (0.29), **2** (0.26), **Zn1** (0.065), **Zn2** (0.072). [i] Ar is 4-[2-(trimethylsilyl)ethoxycarbonyl]phenyl. [j] The same value was obtained from fluorescence and transient absorption measurements in toluene; the lifetime is 0.6 ns in benzonitrile (average from fluorescence and transient absorption measurements).

The lifetimes of the lowest excited singlet states were measured using fluorescence techniques and, in some cases, by time-resolved absorption spectroscopy as well. The results are listed in Table 1. The excited-state lifetime (τ) of each Zn oxochlorin **Oxo-Zn1**−**Oxo-Zn4** is in the range of 0.5−0.7 ns, which is on average 4-fold shorter than the value of 2.0−2.4 ns for **ZnTPP** and related Zn porphyrins.[43,48,49] The lifetime of 3 ns for **Oxo-Mg1** is about 3-fold shorter than that of ∼10 ns for **MgTPP**[44] and other Mg porphyrins.[43] On the other hand, each of the corresponding Fb oxochlorins **Oxo-Fb1**−**Oxo-Fb4** has a lifetime in the range 7.4−8.9 ns, which is only modestly reduced from the lifetime of ∼13 ns for **FbTPP** and related Fb porphyrins.[43,48,49] In general, the excited-state lifetime of each Zn oxochlorin is approximately 2-fold shorter than that of the corresponding chlorin, while the Fb oxochlorins have lifetimes more comparable to their chlorin counterparts (Table 1). The excited-state lifetimes measured here are generally in good agreement with the limited number of values determined previously for related chlorins and oxochlorins.[26,27,45−47]

Knowledge of the excited-singlet-state lifetime (τ) and fluorescence quantum yield (Φ_f) for each chlorin and oxochlorin allows calculation of the natural radiative rate constant (k_{rad}) via eqs 1−3.

$$\tau = (k_{rad} + k_{ic} + k_{isc})^{-1} \quad (1)$$

$$\Phi_f = k_{rad}(k_{rad} + k_{ic} + k_{isc})^{-1} \quad (2)$$

$$k_{rad} = \Phi_f/\tau \quad (3)$$

Here, k_{ic} and k_{isc} are the rate constants by which the excited singlet state decays by internal conversion to the ground state and intersystem crossing to the excited triplet state, the two processes competing with fluorescence emission in the chromophores. The radiative rate constant is proportional to the fluorescence intensity and to the total oscillator strength of the absorption bands associated with transitions from the ground to lowest energy (Q_y) excited state (via the relationship of the respective Einstein coefficients). Indeed, for each compound, a second measure of k_{rad} was obtained by integration through the $Q_y(1,0)$ and $Q_y(0,0)$ absorption bands using the measured extinction coefficients (Experimental Section) and the Strickler−Berg relationship as implemented in the program PhotochemCad.[50] The k_{rad} values determined from the absorption spectrum are generally in reasonable agreement with those obtained using the fluorescence yield and excited-state lifetime data (eq 3) considering the errors associated with each method.

From Table 1, it is seen that the Zn chlorins and the Zn oxochlorins have an average radiative rate constant (k_{rad}) of ∼(15 ns)$^{-1}$. This value is 4-fold greater than the

(45) Gradyushko, A. T.; Sevchenko, A. N.; Solovyov, K. N.; Tsvirko, M. P. *Photochem. Photobiol.* **1970**, *11*, 387−400.
(46) (a) Grewer, Ch.; Schermann, G.; Schmidt, R.; Völcker, A.; Brauer, H.-D.; Meier, A.; Montforts, F.-P. *J. Photochem. Photobiol. B*: *Biol.* **1991**, *11*, 285−293. (b) Pandey, R. K.; Sumlin, A. B.; Constantine, S.; Aoudia, M.; Potter, W. R.; Bellnier, D. A.; Henderson, B. W.; Rodgers, M. A.; Smith, K. M.; Dougherty, T. J. *Photochem. Photobiol.* **1996**, *64*, 194−204. (c) Zenkevich, E.; Sagun, E.; Knuykshto, V.; Shulga, A.; Mironov, A.; Efremova, O.; Bonnett, R.; Songca, S. P.; Kassem, M. *J. Photochem. Photobiol. B*: *Biol.* **1996**, *33*, 171−180. (d) Bonnett, R.; Charlesworth, P.; Djelal, B. D.; Foley, S.; McGarvey, D. J.; Truscott, T. G. *J. Chem. Soc., Perkin Trans. 2* **1999**, 325−328.
(47) Papkovsky, D. B.; Ponomarev, G. V.; Wolfbeis, O. S. *Spectrochim. Acta A* **1996**, *52*, 1629−1638.
(48) Hsiao, J.-S.; Krueger, B. P.; Wagner, R. W.; Johnson, T. E.; Delaney, J. K.; Mauzerall, D. C.; Fleming, G. R.; Lindsey, J. S.; Bocian, D. F.; Donohoe, R. J. *J. Am. Chem. Soc.* **1996**, *118*, 11181−11193.
(49) Li, F.; Gentemann, S.; Kalsbeck, W. A.; Seth, J.; Lindsey, J. S.; Holten, D.; Bocian, D. F. *J. Mater. Chem.* **1997**, *7*, 1245−1262.
(50) Du, H.; Fuh, R.-C. A.; Li, J.; Corkan, L. A.; Lindsey, J. S. *Photochem. Photobiol.* **1998**, *68*, 141−142.

average radiative rate constant of ~(60 ns)$^{-1}$ for metalloporphyrins.[40,42] In analogy, the average value of k_{rad} ~ (30 ns)$^{-1}$ for the Fb chlorins **1**−**4** or ~(60 ns)$^{-1}$ for the Fb oxochlorins **Oxo-1**−**Oxo-4** are approximately 4-fold or 2-fold greater, respectively, than the average value of k_{rad} ~(120 ns)$^{-1}$ for Fb porphyrins.[40,42] These differences are obviously reflected in the strength of the long-wavelength (Q_y) absorption band of the chlorins and oxochlorins compared to the visible-region transitions of the porphyrins.

The strong red-region absorption of the chlorins and oxochlorins represents an advantage compared to the porphyrins in multi-chromophore arrays for light-harvesting applications due to (1) increased utilization of the solar spectrum and (2) increased through-space contribution to inter-pigment energy transfer (depending on the subunits and architecture) due to enhanced transition−dipole transition−dipole coupling. On the other hand, the chlorins and oxochlorins have shortened excited-state lifetimes (and diminished fluorescence yields) compared with porphyrins, with the extent depending on the chromophore. Although longer excited-state lifetimes than ~0.7 ns for the zinc oxochlorin monomers is desirable, efficient energy transfer in arrays comprising these chromophores can be supported depending on the linker and attachment motif and thus the energy-transfer rate. The lifetimes for the free base oxochlorins (~8 ns) provide little if any impediment compared to porphyrins toward energy transfer in arrays. The choice of components in a synthetic light-harvesting array[51] is often a compromise among a number of factors.[52] In terms of absorption, fluorescence, and excited-state decay characteristics, the oxochlorins represent a step forward in extending the properties of porphyrins while attempting to maintain a good balance of properties.

3. Time-Resolved Absorption Spectra. Figure 3 shows representative transient absorption spectra for **Oxo-Zn4** in toluene acquired using 130-fs 585-nm excitation flashes. Similar results were obtained using excitation at other wavelengths and for this compound in benzonitrile. The spectrum at the early time delay (solid line) can be assigned to the excited singlet state of the oxochlorin. The spectrum is dominated by a feature at ~610 nm that is expected to have equal contributions of bleaching of the $Q_y(0,0)$ ground-state band and $Q_y(0,0)$ stimulated emission, the latter stemming from fluorescence from the excited singlet state stimulated by the white-light probe pulse. The spectra obtained immediately after the flash show a slightly smaller feature at ~610 nm than found in the 30-ps spectrum of Figure 3, likely due to a smaller stimulated emission contribution. The initial spectrum evolves into the one at 30 ps with a time constant of ~10 ps, indicating a possible vibrational/conformational relaxation process within the excited singlet state of the chromophore. The 30-ps spectrum also shows $Q_y(0,1)$ stimulated emission at ~660 nm along with broad transient absorption throughout the visible and near-infrared regions. The bleaching and stimulated emission features are coincident with the bands in the static absorption and fluorescence spectra for this compound (Figure 2D).

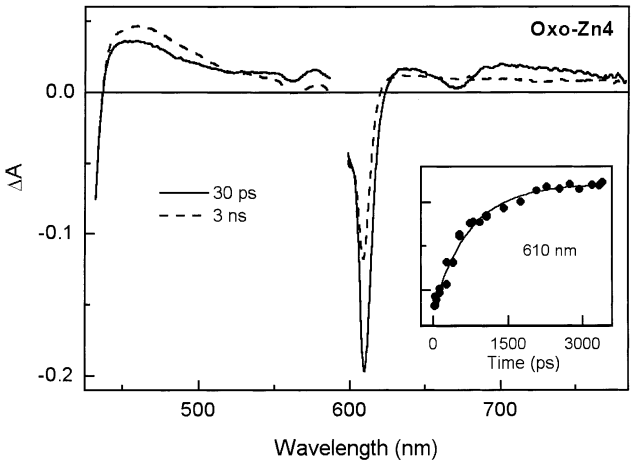

FIGURE 3. Transient absorption spectra at two time delays after excitation of **Oxo-Zn4** in toluene with a 130-fs 585-nm excitation flash. The inset shows a kinetic trace at 610 nm and a single-exponential fit giving with time constant of 720 ± 50 ps; data before and during the instrument response have been deleted for clarity.

As time progresses, the stimulated emission contributions decay, but the $Q_y(0,0)$ ground-state bleaching remains (3.5 ns spectrum in Figure 3, dashed line). These changes are expected for the (nonfluorescent) lowest excited triplet state of **Oxo-Zn4** formed by intersystem crossing from the lowest excited singlet state (the Q_y excited state). The larger transient absorption near 450 nm (i.e., just to longer wavelengths than the Soret bleaching) for the excited triplet versus excited singlet state is analogous to the situation for zinc porphyrins such as ZnTPP.[53] The spectral evolution for **Oxo-Zn4** occurs with a time constant of 720 ± 50 ps in toluene (Figure 3 inset) and 750 ± 70 ps in benzonitrile (not shown), in agreement with the values determined by fluorescence detection (Table 1). Comparison of the magnitude of the bleaching at ~610 nm at long times (relative to the broad transient absorption) and the combined (50/50) bleaching and stimulated emission at early times indicates that very little of the excited singlet state decays to the ground state (by fluorescence and internal conversion). Accordingly, the yield of intersystem crossing to give the excited triplet state is high (likely >70%). This situation is analogous to that for porphyrins, where triplet yields are typically 80−90% for Fb and closed-shell metal chelates.[40,45,54]

4. Resonance Raman Spectra. The high-frequency regions of the Soret-excitation (λ_{ex} = 413 nm) and Q_y-excitation (λ_{ex} = 610 nm) resonance Raman spectra of **Cu1** and **Oxo-Cu1** are shown in Figure 4. The spectra

(51) Burrell, A. K.; Officer, D. L.; Plieger, P. G.; Reid, D. C. W. *Chem. Rev.* **2001**, *101*, 2751−2796.

(52) (a) Tomizaki, K.-Y.; Loewe, R. S.; Kirmaier, C.; Schwartz, J. K.; Retsek, J. L.; Bocian, D. F.; Holten, D.; Lindsey, J. S. *J. Org. Chem.* **2002**, *67*, in press. (b) Wagner, R. W.; Lindsey, J. S. *Pure Appl. Chem.* **1996**, *68*, 1373−1380. (c) Wagner, R. W.; Lindsey, J. S. *Pure Appl. Chem.* **1998**, *70 (8)*, p. i.

(53) Rodriguez, J.; Kirmaier, C.; Holten, D. *J. Am. Chem. Soc.* **1989**, *111*, 6500−6506.

(54) (a) Hurley, J. K.; Sinai, N.; Linschitz, H. *Photochem. Photobiol.* **1983**, *38*, 9−14. (b) Kajii, Y.; Obi, K.; Tanaka, I.; Tobita, S. *Chem. Phys. Lett.* **1984**, *111*, 347−349. (c) Kikuchi, K.; Kurabayashi, Y.; Kokubun, H.; Kaizu, Y.; Kobayashi, H. *J. Photochem. Photobiol. A*: *Chem.* **1988**, *45*, 261−263. (d) Bonnett, R.; McGarvey, D. J.; Harriman, A.; Land, E. J.; Truscott, T. G.; Winfield, U.-J. *Photochem. Photobiol.* **1988**, *48*, 271−276.

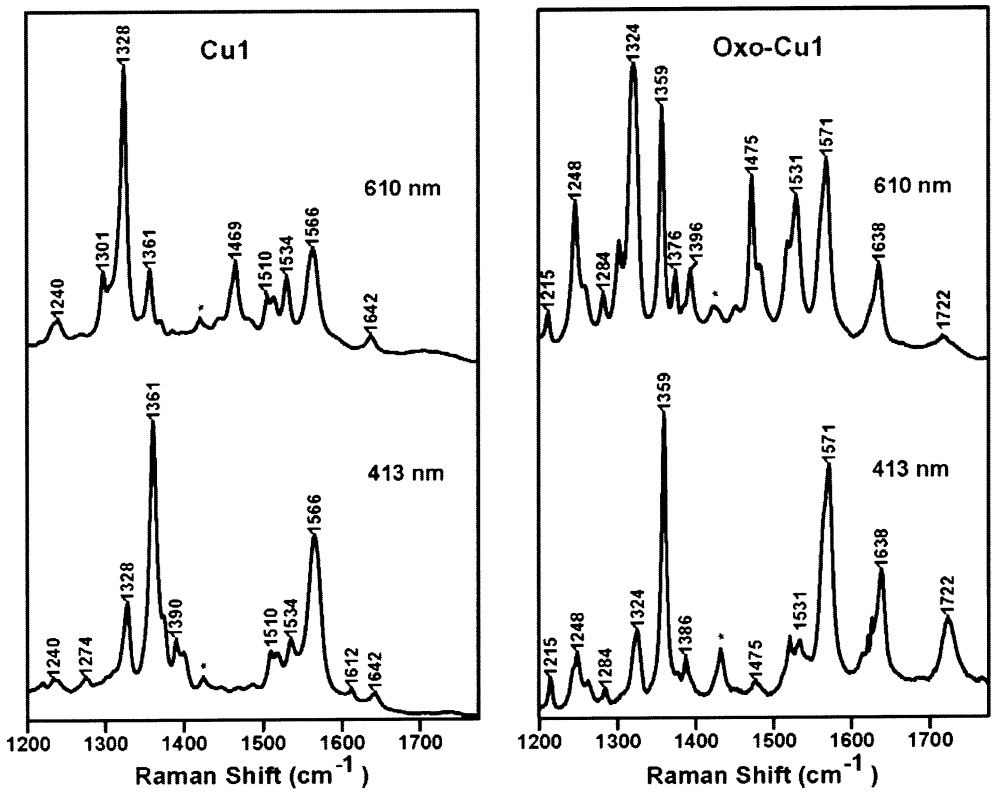

FIGURE 4. High-frequency regions of the Soret-excitation (λ_{ex} = 413 nm) and Q_y-excitation (λ_{ex} = 610 nm) resonance Raman spectra of **Cu1** and **Oxo-Cu1**. The bands marked by asterisks are due to the solvent (CH_2Cl_2).

observed for **Cu2**/**Cu4** and **Oxo-Cu2**/**Oxo-Cu4** (not shown) are similar to those of **Cu1** and **Oxo-Cu1**, respectively. Note that the resonance Raman spectra were acquired for the Cu complexes because this metal causes quenching of the fluorescence from the Q_y state. This fluorescence compromises the acquisition of Q_y-excitation resonance Raman spectra of Zn, Mg, or Fb complexes in solution. The scattering characteristics for the chlorins and oxochlorins are generally similar to those that have been previously reported for these types of macrocycles.[55,56] In general, the resonance Raman spectra of the chlorins and oxochlorins are much richer than those of porphyrins. This spectral richness arises because of the lower symmetry of the chlorins (and oxochlorins), which results primarily from saturation of one of the β-pyrrole bonds.

A key spectral feature that distinguishes the oxochlorins from the chlorins is the band due to the stretching vibration of the keto group ($\nu_{C=O}$).[56] The $\nu_{C=O}$ mode is observed at ~1722 cm^{-1} and is strongly resonance enhanced with Soret excitation (Figure 4, right panel, bottom trace). The $\nu_{C=O}$ mode is much less strongly enhanced with Q_y excitation. The relatively weak Q_y enhancement is due to the fact that the keto group of the oxochlorin is at the 17-position, thus lying primarily along the *x*-axis of the macrocycle (Chart 1).[55,56] In contrast, the $\nu_{C=O}$ vibration of the keto group of chlorophyll is strongly enhanced with Q_y excitation.[55,56] In the case of chlorophyll, the keto group is not appended to the saturated pyrrole ring of the macrocycle, but rather is attached to the 13-position as part of an exocyclic five-membered ring; the keto group thus lies along the *y*-axis of the chlorophyll chromophore. Finally, an additional vibrational feature that is observed for **Cu4** and **Oxo-Cu4** is the stretching vibration of the ethyne group ($\nu_{C\equiv C}$). The $\nu_{C\equiv C}$ mode is observed at ~2215 cm^{-1} and is most strongly enhanced with Soret excitation (not shown). This mode is also resonance enhanced in metalloporphyrins bearing an ethyne group on a phenyl substituent.[57]

5. Electrochemistry. The oxidation potentials of selected chlorins and oxochlorins were determined as described previously.[43] The $E_{1/2}$ value for **Zn1** is 0.35 V whereas that for **Oxo-Zn1** is 0.59 V (vs Ag/Ag^+; $E_{1/2}(Fc/Fc^+)$ = 0.19 V). Turning to the analogues in which the *p*-tolyl and mesityl groups are replaced by pentafluorophenyl rings, the $E_{1/2}$ value of **Zn2** is 0.55 V whereas that for **Oxo-Zn2** is 0.78 V (Table 1). These results indicate that a single oxo group imparts essentially the same electron-withdrawing effect on the chlorin as achieved with two *meso*-pentafluorophenyl groups. This result is explainable on the basis of the

(55) (a) Schick, G. A.; Bocian, D. F. *Biochim. Biophys. Acta* **1987**, *895*, 127−154. (b) Boldt, N. J.; Donohoe, R. J.; Birge, R. R.; Bocian, D. F. *J. Am. Chem. Soc.* **1987**, *109*, 2284−2298.

(56) (a) Andersson, L. A.; Loehr, T. M.; Wu, W.; Chang, C. K.; Timkovich, R. *FEBS Lett.* **1990**, *267*, 285−288. (b) Mylrajan, M.; Andersson, L. A.; Loehr, T. M.; Wu, W.; Chang, C. K. *J. Am. Chem. Soc.* **1991**, *113*, 5000−5005.

(57) (a) Seth, J.; Palaniappan, V.; Johnson, T. E.; Prathapan, S.; Lindsey, J. S.; Bocian, D. F. *J. Am. Chem. Soc.* **1994**, *116*, 10578−10592. (b) Seth, J.; Palaniappan, V.; Wagner, R. W.; Johnson, T. E.; Lindsey, J. S.; Bocian, D. F. *J. Am. Chem. Soc.* **1996**, *118*, 11194−11207. (c) Strachan, J.-P.; Gentemann, S.; Seth, J.; Kalsbeck, W. A.; Lindsey, J. S.; Holten, D.; Bocian, D. F. *J. Am. Chem. Soc.* **1997**, *119*, 11191−11201. (d) Strachan, J.-P.; Gentemann, S.; Seth, J.; Kalsbeck, W. A.; Lindsey, J. S.; Holten, D.; Bocian, D. F. *Inorg. Chem.* **1998**, *37*, 1191−1201.

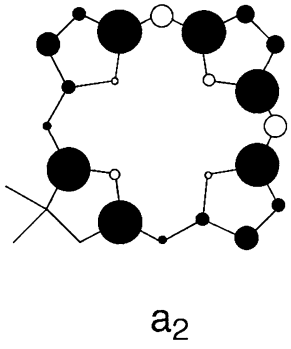

FIGURE 5. Highest occupied molecular orbital of a chlorin (a_2 orbital). Note the very large electron density at the site adjacent to the methylene unit in the reduced ring.

electron density distribution in the HOMO of the chlorin, which is characterized by small orbital coefficients at the meso-positions (Figure 5).[58−60] The ability to substantially alter the electrochemical potential of the chlorins by introduction of a single oxo group in the reduced ring enables the meso and β-positions to be employed for synthetic handles and solubilizing groups. Further tuning of potentials can be achieved by formation of the Mg chelate, which shifts the potentials to less positive values compared with those of the Zn chelates (compare **Oxo-Mg1** or **Oxo-Mg2** versus the corresponding Zn chelates). Thus, our strategy to tune the redox properties of the chlorin macrocycle by the incorporation of an oxo group in the reduced ring is superior to the incorporation of electronegative substituents at the meso positions.

Conclusions

Oxochlorins have absorption spectral features nearly identical to those of chlorins, but are more resistant to oxidation. Indeed, an oxochlorin exhibits an oxidation potential similar to that of the corresponding porphyrin. On the other hand, the fluorescence yield of an oxochlorin is diminished relative to that of a chlorin, again resembling that of a porphyrin. In general, oxochlorins have spectral features resembling chlorins but the oxidation and fluorescence yield properties resembling a porphyrin. The lifetime of the lowest excited singlet state of Zn oxochlorins (∼0.7 ns) is roughly 2- or 4-fold shorter than that of Zn chlorins or porphyrins, respectively, whereas the lifetimes for Fb chlorins and oxochlorins (∼8 ns) are only modestly (∼40%) shorter than for a porphyrin. These excited-state lifetimes are sufficiently long to support efficient excited-state energy transfer in arrays utilizing chlorins or oxochlorins. The ability to prepare C-alkylated oxochlorin building blocks in a rational manner, by way of the corresponding chlorins, sets the stage for the preparation of diverse multipigment arrays containing oxochlorin components. The spectral and electronic studies reported herein of chlorin and oxochlorin monomers provide the foundation for designing monomers with desired properties for incorporation into such arrays and in turn for characterizing the properties of these multichromophore architectures.

Experimental Section

A. Synthetic Procedures. 1. General Procedures. All ^{1}H NMR spectra (300 or 400 MHz) were obtained in $CDCl_3$ unless noted otherwise. IR spectra were obtained from films evaporated from CH_2Cl_2 on a NaCl window. Basic alumina (60−325 mesh, activity grade I) and neutral alumina (80−200 mesh) were obtained from Fisher Scientific. Activity grade V alumina was prepared from grade I alumina.[49] Chlorins and oxochlorins were analyzed by laser desorption mass spectrometry without a matrix (LD-MS) or with the matrix POPOP (MALDI-MS).[61] Fast atom bombardment mass spectrometry (FAB-MS) data are reported for the molecule ion or protonated molecule ion. Column chromatography was performed with flash silica (Baker).

2. Solvents. THF was distilled from sodium benzophenone ketyl as required. Toluene was distilled from CaH_2. CH_3CN (A.C.S. grade) for use in the condensation process was distilled from CaH_2 and stored over powdered molecular sieves. Nitromethane was stored over $CaCl_2$. Anhydrous methanol was prepared by drying over CaH_2 for 12 h followed by distillation. All other solvents were used as received.

3. Noncommercial Compounds. The chlorins **Zn1**−**Zn5**,[3] **1** and **2**,[8] and Eastern half **11-OH**[8] were prepared as described in the literature.

Chlorin Hydroxylation Using Basic Alumina, Exemplified for Zn(II)-17,18-dihydro-18,18-dimethyl-5-(4-methylphenyl)-10-mesityl-17-oxoporphyrin (Oxo-Zn1). A mixture of **Zn1** (100 mg, 0.163 mmol) and basic alumina (activity I, 7.0 g) in 8 mL of toluene was stirred at 60 °C for 22 h exposed to air. TLC (silica, CH_2Cl_2/ethyl acetate, 19:1) showed three components: a blue component (R_f = 0.82; **Zn1**), a green component (R_f = 0.38; **Oxo-Zn1**), and a blue component (R_f = 0.15; **HO-Zn1**). The alumina was removed by filtration and washed (CH_2Cl_2/CH_3OH, 19:1) until the washings were colorless. The filtrate was concentrated and the residue was chromatographed (silica, CH_2Cl_2), affording **Zn1** (2.0 mg, 2%) as the first fraction and **Oxo-Zn1** (23.4 mg, 23%) as the second fraction. Further elution (CH_2Cl_2/ethyl acetate, 49:1) gave hydroxychlorin **HO-Zn1** (52.9 mg, 52%). Data for **Oxo-Zn1**: IR 1717 cm^{-1} (br); ^{1}H NMR δ 1.82 (s, 6H), 2.03 (s, 6H), 2.59 (s, 3H), 2.67 (s, 3H), 7.22 (s, 2H), 7.50 (d, J = 8.1 Hz, 2H), 7.98 (d, J = 8.1 Hz, 2H) 8.46 (d, J = 4.2 Hz, 1H), 8.54 (d, J = 4.2 Hz, 1H) 8.64 (d, J = 4.2 Hz, 1H), 8.83 (d, J = 4.2 Hz, 1H), 8.80−8.95 (m, 2H), 8.94 (s, 1H), 9.55 (s, 1H); LD-MS obsd 622.16; FAB-MS obsd 624.1869, calcd 624.1868 ($C_{38}H_{32}N_4OZn$); λ_{abs} 423 (log ϵ = 5.32), 563 (3.82), 609 (4.60) nm; λ_{em} 609, 650, 669 nm. Data for Zn(II)-17,18-dihydro-18,18-dimethyl-17-hydroxy-5-(4-methylphenyl)-10-mesitylporphyrin (**HO-Zn1**): LD-MS obsd 625.01, calcd 626.01 ($C_{38}H_{34}N_4OZn$).

Conversion of Hydroxychlorin (HO-Zn1) to Oxochlorin (Oxo-Zn1) using DDQ. To a solution of **HO-Zn1** (96.6 mg, 0.154 mmol) in 80 mL of toluene was added DDQ (52.4 mg, 0.231 μmol). The mixture was stirred for 5 min, 2 mL of triethylamine was added, and the solvent was removed under reduced pressure. The residue was immediately chromatographed (silica, CH_2Cl_2), affording a purple solid (45.6 mg, 47%).

Two-Step Procedure for the Synthesis of Oxochlorins (Oxo-Zn1). A mixture of **Zn1** (50.0 mg, 81.7 μmol) and basic alumina (activity I, 3.0 g) in 4 mL of toluene was stirred at 50 °C for 6.5 h exposed to air. The alumina was removed by filtration and washed (CH_2Cl_2/CH_3OH, 19:1) until the wash-

(58) Fajer, J.; Davis, M. S. In *The Porphyrins*; Dolphin, D., Ed.; Academic Press: New York, 1979; Vol. IV, pp 197−256.
(59) Ozawa, S.; Watanabe, Y.; Morishima, I. *J. Am. Chem. Soc.* **1994**, *116*, 5832−5838.
(60) (a) Parusel, A. B. J.; Ghosh, A. *J. Phys. Chem. A* **2000**, *104*, 2504−2507. (b) Ghosh, A. *J. Phys. Chem. B* **1997**, *101*, 3290−3297.
(61) (a) Fenyo, D.; Chait, B. T.; Johnson, T. E.; Lindsey, J. S. *J. Porphyrins Phthalocyanines* **1997**, *1*, 93−99. (b) Srinivasan, N.; Haney, C. A.; Lindsey, J. S.; Zhang, W.; Chait, B. T. *J. Porphyrins Phthalocyanines* **1999**, *3*, 283−291.

ings were colorless. The filtrate was concentrated, and the residue was dissolved in toluene (40 mL). DDQ (37.0 mg, 163 μmol) was added, the mixture was stirred for 5 min, 1 mL of triethylamine was added, and the solvent was removed under reduced pressure. The residue was immediately chromatographed (silica, CH_2Cl_2), affording a purple solid as the only isolable product (27.2 mg, 53%).

Zn(II)-17,18-dihydro-18,18-dimethyl-17-oxo-5,10-bis-(pentafluorophenyl)porphyrin (Oxo-Zn2). Following the procedure for preparing **Oxo-Zn1**, a mixture of chlorin **Zn2** (21.0 mg, 28.5 μmol) and basic alumina (activity I, 1.4 g) in 0.75 mL of toluene was stirred for 120 h. Solvent was removed under reduced pressure, and the residue was washed (CH_2Cl_2/CH_3OH, 19:1) until the washings were colorless. The filtrate was removed, and the residue was chromatographed (silica). Elution with hexanes/CH_2Cl_2 (1:4) gave **Zn2** (8.0 mg, 38%); elution with CH_2Cl_2 gave **Oxo-Zn2** (3.0 mg, 14%); elution with CH_2Cl_2/ethyl acetate (49:1) gave hydroxychlorin **HO-Zn2** (7.0 mg, 33%). LD-MS data for **HO-Zn2**: obsd 752.72 calcd 750.05 ($C_{34}H_{16}F_{10}N_4OZn$). DDQ (4.2 mg, 18 μmol) was added to a solution of **HO-Zn2** (7.0 mg, 9.3 μmol) in toluene (200 μL). The mixture was stirred for 45 min. Triethylamine (100 μL) was added, and the solvent was removed under reduced pressure. The residue was chromatographed (silica, CH_2Cl_2), affording a green solid (5.2 mg, 74%): IR 1719 cm^{-1}; ^{1}H NMR δ 1.94 (s, 6H), 8.56 (d, J = 4.8 Hz, 1H), 8.61 (d, J = 4.8 Hz, 1H), 8.72−8.76 (m, 2H) 9.03 (d, J = 4.8 Hz, 1H), 9.07 (d, J = 4.8 Hz, 1H), 9.08 (s, 1H), 9.60 (s, 1H); LD-MS obsd 746.43; FAB-MS obsd 748.0339, calcd 748.0299 ($C_{34}H_{14}F_{10}N_4OZn$); λ_{abs} 423 (log ϵ = 5.23), 567 (3.80), 613 (4.54) nm; λ_{em} 614, 653, 671 nm.

Zn(II)-17,18-dihydro-18,18-dimethyl-5-(4-methylphenyl)-10-[4-[2-(trimethylsilyl)ethoxycarbonyl]phenyl]-17-oxoporphyrin (Oxo-Zn3). A mixture of **Zn3** (25.0 mg, 35.0 μmol) and basic alumina (activity I, 1.5 g) in 2 mL of toluene was stirred for 4 h at 50 °C exposed to air. After standard workup, the residue was dissolved in 1.5 mL of toluene, and DDQ (19.9 mg, 87.5 μmol) was added. Standard workup and chromatography [silica, ethyl acetate/CH_2Cl_2 (1:5)] gave a bluish-purple solid (8.2 mg, 31%): ^{1}H NMR δ 0.17 (s, 9H), 1.22−1.27 (m, 2H), 2.04 (s, 6H), 2.68 (s, 3H), 4.47−4.54 (m, 2H), 7.52 (d, J = 8.0 Hz, 2H), 7.97 (d, J = 8.0 Hz, 2H), 8.15 (d, J = 8.0 Hz, 2H), 8.30 (d, J = 8.0 Hz, 2H), 8.54 (d, J = 4.4 Hz, 1H), 8.61 (d, J = 4.4 Hz, 1H), 8.72 (d, J = 4.4 Hz, 1H), 8.86 (d, J = 4.4 Hz, 1H), 8.93 (d, J = 4.4 Hz, 1H), 8.97 (d, J = 4.4 Hz, 1H), 8.98 (s, 1H), 9.56 (s, 1H); LD-MS obsd 727.45; FAB-MS obsd 726.2002, calcd 726.2005 ($C_{41}H_{38}N_4O_3SiZn$); λ_{abs} 425 (log ϵ = 5.39), 564 (3.96), 610 (4.62) nm; λ_{em} 610, 651, 669 nm.

Zn(II)-5-(3,5-di-*tert*-butylphenyl)-10-(4-ethynylphenyl)-17,18-dihydro-18,18-dimethyl-17-oxoporphyrin (Oxo-Zn4). A mixture of **Zn4** (50.0 mg, 72.2 μmol) and basic alumina (activity I, 3.0 g) in 4 mL of toluene was stirred for 8 h at 50 °C. After standard workup, the residue was dissolved in 40 mL of toluene, and DDQ (32.7 mg, 144 μmol) was added. Standard workup and chromatography (silica, CH_2Cl_2) gave a bluish-purple solid (30.4 mg, 60%): ^{1}H NMR δ 1.51 (s, 18H), 2.01 (s, 6H), 3.30 (s, 1H), 7.77 (t, J = 1.6 Hz, 1H), 7.84 (d, J = 8.4 Hz, 2H), 7.95 (d, J = 1.6 Hz, 2H), 8.07 (d, J = 8.4 Hz, 2H), 8.59 (d, J = 4.4 Hz, 1H), 8.64 (d, J = 4.4 Hz, 1H), 8.76 (d, J = 4.4 Hz, 1H), 8.88 (d, J = 4.4 Hz, 1H), 8.94 (d, J = 4.4 Hz, 1H), 8.97 (s, 1H), 8.98 (d, J = 4.4 Hz, 1H), 9.51 (s, 1H); LD-MS obsd 704.88; FAB-MS obsd 704.2507, calcd 704.2494 ($C_{44}H_{40}N_4OZn$); λ_{abs} 426 (log ϵ = 5.40), 564 (4.01), 610 (4.73) nm; λ_{em} 610, 650, 668 nm.

Zn(II)-5-(3,5-di-*tert*-butylphenyl)-17,18-dihydro-10-(4-iodophenyl)-18,18-dimethyl-17-oxoporphyrin (Oxo-Zn5). A mixture of **Zn5** (75.0 mg, 94.4 μmol) and basic alumina (activity I, 4.5 g) in 6 mL of toluene was stirred for 5 h at 50 °C. After standard workup, the residue was dissolved in 60 mL of toluene, and DDQ (42.9 mg, 189 μmol) was added. Standard workup and chromatography [silica, hexanes/CH_2Cl_2 (1:3)] gave a bluish purple solid (49.8 mg, 65%): ^{1}H NMR δ 1.51 (s, 18H), 2.06 (s, 6H), 7.77 (t, J = 1.6 Hz, 1H), 7.84 (d, J = 8.4 Hz, 2H), 7.94 (d, J = 1.6 Hz, 2H), 8.05 (d, J = 8.4 Hz, 2H), 8.60 (d, J = 4.4 Hz, 1H), 8.63 (d, J = 4.4 Hz, 1H), 8.78 (d, J = 4.4 Hz, 1H), 8.88 (d, J = 4.4 Hz, 1H), 8.94 (d, J = 4.4 Hz, 1H), 8.98 (s, 1H), 9.00 (d, J = 4.4 Hz, 1H), 9.61 (s, 1H); LD-MS obsd 804.57; FAB-MS obsd 806.1472, calcd 806.1460 ($C_{42}H_{39}IN_4OZn$); λ_{abs} 425 (log ϵ = 5.25), 563 (3.84), 609 (4.49) nm; λ_{em} 610, 649, 668 nm.

2-(2-Nitroethyl)pyrrole (6). Pyrrole-2-carboxaldehyde (2.85 g, 30.0 mmol) was dissolved in 90 mL of dry methanol and treated with nitromethane (4.85 mL, 90.0 mmol), sodium acetate (2.71 g, 33.0 mmol), and methylamine hydrochloride (2.23 g, 33.0 mmol). Stirring at room temperature for 12 h afforded a yellow/brown mixture. DMF (60 mL) and methanol (50 mL) were added to the reaction mixture. Sodium borohydride (3.97 g, 105 mmol) was added portionwise. The reaction mixture was stirred at room temperature for 1 h, neutralized with acetic acid (~5 mL), and evaporated. The mixture was dissolved in dichloromethane (150 mL) and washed with water. The organic layer was dried (Na_2SO_4), concentrated, and chromatographed (silica, CH_2Cl_2) to give an orange oil (2.79 g, 66%). The ^{1}H NMR spectrum and the ^{13}C NMR spectrum were identical with the literature data:[8] IR 3406, 1552, 1380 cm^{-1}; Anal. Calcd for $C_6H_8N_2O_2$: C, 51.42; H, 5.75; N, 19.99. Found: C, 51.38; H, 5.71; N, 19.92.

1-Cyclohexylidene-2-propanone (7). Following a standard procedure,[37] a solution of KOH (840 mg, 15.0 mmol) in ethanol/H_2O (30.0 mL, 4:1) was treated with cyclohexanone (1.04 mL, 10.0 mmol). Stirring at room temperature for 28 h afforded a light brown mixture. The mixture was extracted with petroleum ether. The organic layer was washed with water, dried (Na_2SO_4), and evaporated. The residue was purified by column chromatography (silica, dichloromethane) to give a colorless oil (1.45 g, 95%). Analytical data were consistent with the literature for the title compound prepared via a different route.[38]

1-[1-[1-Nitro-2-(1*H*-pyrrol-2-yl)ethyl]cyclohexyl]propan-2-one (8). Following a general procedure,[8,32] cesium fluoride (3.58 g, 23.6 mmol, 3.00 molar equiv, freshly dried by heating to 100 °C under vacuum for 1 h and then cooling to room temperature under argon) was placed in a flask under argon. A mixture of **6** (1.10 g, 7.85 mmol) and **7** (7.17 g, 47.1 mmol) in 50 mL of dry acetonitrile was transferred to the flask by cannula. The mixture was heated at 70 °C for 7 h, whereupon the reaction was deemed to be complete by TLC analysis. The reaction mixture was filtered. The filtrate was evaporated and chromatographed [alumina, ethyl acetate/hexanes (1:3)], affording a light yellow oil that solidified upon storing in the freezer (1.11 g, 51%): mp 82 °C; IR 3395, 1712, 1547, 1366 cm^{-1}; ^{1}H NMR δ_1.20−1.98 (m, 10H), 2.18 (s, 3H), 2.63, 2.70 (AB, ^2J = 17.7 Hz, 2H), 3.10 (ABX, ^3J = 2.7 Hz, ^2J = 15.3 Hz, 1H), 3.30 (ABX, ^3J = 11.7 Hz, ^2J = 15.3 Hz, 1H), 5.18 (ABX, ^3J = 2.7 Hz, ^3J = 11.7 Hz, 1H), 5.94−5.98 (m, 1H), 6.07−6.12 (m, 1H), 6.64−6.67 (m, 1H), 8.10−8.22 (br, 1H); ^{13}C NMR δ 21.3, 25.3, 26.2, 30.9, 31.0, 32.2, 40.0, 43.8, 94.6, 107.1, 108.6, 117.7, 126.1, 207.7. Anal. Calcd for $C_{15}H_{22}N_2O_3$: C, 64.73; H, 7.97; N, 10.06. Found: C, 64.46; H, 7.88; N, 10.12.

3-Methyl-1-(1*H*-pyrrol-2-ylmethyl)-2-azaspiro[4.5]dec-2-ene 2-Oxide (9). Following a general procedure,[3] a vigorously stirred solution of **8** (700 mg, 2.51 mmol) in 12 mL of acetic acid and 12 mL of ethanol at 0 °C was treated with Zn dust (4.11 g, 62.8 mmol) in small portions over 5 min. The reaction mixture was stirred at 0 °C for 15 min and then was filtered through Celite. The filtrate was concentrated under high vacuum. The resulting brown solid was purified by column chromatography [silica; packed and eluted with ethyl acetate/CH_2Cl_2 (1:1), then eluted with CH_2Cl_2/methanol (9:1)], affording a brown oil that solidified to brownish crystals on standing at room temperature (498 mg, 81%): mp 109−110 °C; IR 3200, 1216 cm^{-1}; ^{1}H NMR δ 1.25−1.89 (m, 10 H), 2.01 (s, 3H), 2.28−2.44 (m, 2H), 3.00 (ABX, ^3J = 3.7 Hz, ^2J = 16.1 Hz, 1H), 3.17 (ABX, ^3J = 6.6 Hz, ^2J = 16.1 Hz, 1H), 3.83−3.91

(m, 1H), 5.92−5.96 (m, 1H), 6.04−6.09 (m, 1H), 6.66−6.71 (m, 1H), 10.35−10.60 (br, 1H); ^{13}C NMR δ 13.2, 22.4, 25.6, 25.7, 30.8, 30.9, 37.0, 40.1, 42.8, 81.3, 106.4, 107.2, 117.3, 128.3, 146.1; FAB-MS obsd 247.1813, calcd 247.1810 ($C_{15}H_{22}N_2O$).

3-Methyl-1-(1*H*-pyrrol-2-ylmethyl)-2-azaspiro[4.5]dec-2-ene (10). Following a procedure for the deoxygenation of tetrahydrodipyrrin *N*-oxides,[3] $TiCl_4$ (1.51 mL, 13.7 mmol) was slowly added with stirring to dry THF (30 mL) under argon at 0 °C. To the resulting yellow solution was slowly added $LiAlH_4$ (370 mg, 9.75 mmol). The resulting black mixture was stirred at room temperature for 15 min, and then triethylamine (12.2 mL, 87.8 mmol) was added. The black mixture was then poured into a solution of **9** (480 mg, 1.95 mmol) in dry THF (20 mL). The mixture was stirred for 30 min at room temperature, and then water (25 mL) was added. The mixture was filtered. The filtrate was extracted with CH_2Cl_2. The organic layer was dried (Na_2SO_4) and evaporated under reduced pressure. The resulting yellow oil was purified by chromatography (silica, ethyl acetate) to give a pale yellow oil, which solidified to a pale yellow solid on cooling (228 mg, 51%): mp 54−55 °C; IR 3358, 1648 cm^{-1}; ^{1}H NMR δ 1.16−1.71 (m, 10H), 2.04 (s, 3H), 2.31, 2.46 (AB, ^2J = 17.6 Hz, 2H), 2.53 (ABX, ^3J = 11.0 Hz, ^2J = 14.7 Hz, 1H), 2.85 (ABX, ^3J = 2.9 Hz, ^2J = 14.7 Hz, 1H), 3.63−3.73 (m, 1H), 5.92−5.96 (m, 1H), 6.08−6.13 (m, 1H), 6.68−6.73 (m, 1H), 9.70−9.95 (br, 1 H); ^{13}C NMR δ 20.8, 23.6, 24.1, 26.4, 28.4, 31.3, 37.2, 45.9, 49.7, 81.1, 105.5, 107.5, 116.6, 131.9, 174.2; FAB-MS obsd 379.1349, calcd 379.1328 ($C_{18}H_{22}N_2O_5S$).

Spirohexylchlorin Zn12. Following a general procedure,[3] a solution of **11** (140 mg, 0.304 mmol) in 10 mL of anhydrous THF/methanol (4:1) was treated with $NaBH_4$ (115 mg, 3.04 mmol). The resulting Eastern half (**11-OH**) was dissolved in 3 mL of anhydrous CH_3CN, and then the Western half (**10**, 70.0 mg, 0.304 mmol) and TFA (23.4 μL, 0.304 mmol) were added. The solution was stirred at room temperature for 30 min. The reaction was quenched with 10% aqueous $NaHCO_3$ (50 mL). The resulting mixture was extracted with distilled CH_2Cl_2. The combined organic layers were washed with water, dried (Na_2SO_4), and concentrated in vacuo without heating. The residue, which contains the crude tetrahydrobilene-*a*, was dissolved in 30 mL of toluene, to which AgOTf (137 mg, 0.534 mmol), $Zn(OAc)_2$ (490 mg, 2.67 mmol), and 2,2,6,6-tetramethylpiperidine (447 μL, 2.67 mmol) were added. The reaction mixture was refluxed for 24 h. The reaction mixture was concentrated and chromatographed [silica, hexanes/CH_2Cl_2 (2:1)], affording a blue solid (37 mg, 19%): ^{1}H NMR δ 0.80−2.70 (m, 22H), 4.55 (s, 2H), 7.20 (s, 2H), 7.47 (d, J = 8.1 Hz, 2H), 7.95 (d, J = 8.1 Hz, 2H), 8.22 (d, J = 4.5 Hz, 1H), 8.36 (d, J = 4.5 Hz, 1H), 8.48 (d, J = 4.5 Hz, 1H), 8.54−8.67 (m, 5H); LD-MS obsd 649.89; FAB-MS obsd 650.2399, calcd 650.2388 ($C_{41}H_{38}N_4Zn$); λ_{abs} 412, 610 nm; λ_{em} 610, 654, 666 nm.

Spirohexyloxochlorin Oxo-Zn12. A mixture of **Zn12** (25 mg, 38 μmol) and basic alumina (activity I, 1.7 g) in 3 mL of toluene was stirred at 85 °C for 15 h. After standard workup, the residue was dissolved in 3 mL of toluene, and DDQ (16.9 mg, 76.1 μmol) was added. Standard workup and chromatography (silica, CH_2Cl_2) gave a bluish-purple solid (5.0 mg, 20%): ^{1}H NMR δ 0.85−2.70 (m, 22H), 7.23 (s, 2H), 7.51 (d, J = 8.1 Hz, 2H), 7.98 (d, J = 8.1 Hz, 2H), 8.22 (d, J = 4.5 Hz, 1H), 8.45 (d, J = 4.5 Hz, 1H), 8.53 (d, J = 4.5 Hz, 1H), 8.80−8.93 (m, 3H), 8.98 (s, 1H), 9.45 (s, 1H); LD-MS obsd 664.70; FAB-MS obsd 664.2198, calcd 664.2181 ($C_{41}H_{36}N_4OZn$); λ_{abs} 424, 611 nm; λ_{em} 611, 651, 669 nm.

17,18-Dihydro-18,18-dimethyl-5-(4-methylphenyl)-10-[4-[2-(trimethylsilyl)ethoxycarbonyl]phenyl]porphyrin (3). A solution of **Zn3** (16.0 mg, 22.4 μmol) in 5 mL of CH_2Cl_2 was treated with a 50-fold excess of TFA. The demetalation was complete in 1 h as confirmed by UV/vis and TLC analyses. Standard workup and chromatography [silica, hexanes/CH_2Cl_2 (1:1)] gave a reddish purple solid (10.8 mg, 74%): ^{1}H NMR δ −1.94 to −1.87 (br, 2H), 0.17 (s, 9H), 1.25−1.32 (m, 2H), 2.06 (s, 6H), 2.67 (s, 3H), 4.53−4.64 (m, 2H), 4.62 (s, 2H), 7.51 (d, J = 7.6 Hz, 2H), 8.00 (d, J = 7.6 Hz, 2H), 8.20 (d, J = 8.0 Hz, 2H), 8.38 (d, J = 8.0 Hz, 2H), 8.40 (d, J = 4.4 Hz, 1H), 8.51 (d, J = 4.4 Hz, 1H), 8.70 (d, J = 4.8 Hz, 1H), 8.78−8.82 (m, 2H), 8.84 (d, J = 4.8 Hz, 1H), 8.88 (s, 1H), 8.97 (s, 1H); LD-MS obsd 649.96; FAB-MS obsd 651.3171, calcd 651.3155 ($C_{41}H_{42}N_4O_2Si$) $[M + H]^+$; λ_{abs} 415 (log ϵ = 5.58), 509 (4.54), 589 (3.09), 640 (4.97) nm; λ_{em} 641, 683, 707 nm.

5-(3,5-Di-*tert*-butylphenyl)-10-(4-ethynylphenyl)-17,18-dihydro-18,18-dimethylporphyrin (4). Treatment of a solution of **Zn4** (22.0 mg, 31.8 μmol) in 10 mL of CH_2Cl_2 with a 50-fold excess of TFA for 1 h followed by standard workup and chromatography [silica, hexanes/CH_2Cl_2 (2:1)] gave a reddish purple solid (12.5 mg, 62%): ^{1}H NMR δ −1.88 to −1.84 (br, 2H), 1.50 (s, 18H), 2.06 (s, 6H), 3.29 (s, 1H), 4.62 (s, 2H), 7.75 (t, J = 1.6 Hz, 1H), 7.84 (d, J = 7.6 Hz, 2H), 7.97 (d, J = 1.6 Hz, 2H), 8.09 (d, J = 7.6 Hz, 2H), 8.44 (d, J = 4.4 Hz, 1H), 8.53 (d, J = 4.4 Hz, 1H), 8.72 (d, J = 4.8 Hz, 1H), 8.80 (d, J = 4.8 Hz, 1H), 8.81−8.85 (m, 2H), 8.87 (s, 1H), 8.96 (s, 1H); LD-MS obsd 627.09; FAB-MS obsd 628.3550, calcd 628.3566 ($C_{44}H_{44}N_4$); λ_{abs} 416 (log ϵ = 5.16), 510 (4.13), 590 (3.67), 641 (4.54) nm; λ_{em} 641, 683, 707 nm.

5-(3,5-Di-*tert*-butylphenyl)-17,18-dihydro-10-(4-iodophenyl)-18,18-dimethylporphyrin (5). Treatment of a solution of **Zn5** (67.6 mg, 85.1 μmol) in 25 mL of CH_2Cl_2 with a 50-fold excess of TFA for 1.5 h followed by standard workup and chromatography [silica, hexanes/CH_2Cl_2 (3:1)] gave a reddish purple solid (43.7 mg, 70%): ^{1}H NMR δ −1.92 to −1.84 (br, 2H), 1.50 (s, 18H), 2.06 (s, 6H), 4.61 (s, 2H), 7.75 (t, J = 1.5 Hz, 1H), 7.86 (d, J = 8.1 Hz, 2H), 7.97 (d, J = 1.5 Hz, 2H), 8.04 (d, J = 8.1 Hz, 2H), 8.44 (d, J = 4.4 Hz, 1H), 8.53 (d, J = 4.4 Hz, 1H), 8.72 (d, J = 5.1 Hz, 1H), 8.79 (d, J = 5.1 Hz, 1H), 8.80−8.86 (m, 2H), 8.87 (s, 1H), 8.96 (s, 1H); LD-MS obsd 729.33; FAB-MS obsd 730.2539, calcd 730.2532 ($C_{42}H_{43}IN_4$); λ_{abs} 416 (log ϵ = 5.19), 510 (4.16), 592 (3.71), 641 (4.59) nm; λ_{em} 641, 683, 708 nm.

17,18-Dihydro-18,18-dimethyl-5-(4-methylphenyl)-10-mesityl-17-oxoporphyrin (Oxo-1). Treatment of a solution of **Oxo-Zn1** (6.2 mg, 9.6 μmol) in 0.4 mL of CH_2Cl_2 with 40 μL of TFA for 2 h followed by standard workup and chromatography [silica, hexanes/CH_2Cl_2 (3:1)] gave a reddish purple solid (5.2 mg, 93%): IR 1723 cm^{-1}; ^{1}H NMR δ −2.32 to −2.23 (br, 1H), −2.23 to −2.17 (br, 1H), 1.85 (s, 6H), 2.11 (s, 6H), 2.63 (s, 3H), 2.70 (s, 3H), 7.55 (d, J = 7.2 Hz, 2H), 8.04 (d, J = 7.2 Hz, 2H), 8.50 (d, J = 4.5 Hz, 2H), 8.58 (d, J = 4.5 Hz, 2H), 8.74 (d, J = 4.5 Hz, 1H), 8.94 (d, J = 4.5 Hz, 1H) 9.08 (d, J = 4.5 Hz, 1H), 9.11 (d, J = 4.5 Hz, 1H) 9.21 (s, 1H), 9.82 (s, 1H); LD-MS obsd 560.08; FAB-MS obsd 562.2753, calcd 562.2733 ($C_{38}H_{34}N_4O$); λ_{abs} 414 (log ϵ = 5.24), 512 (4.10), 545 (3.86), 586 (3.74), 643 (4.31) nm; λ_{em} 643, 685, 713 nm.

17,18-Dihydro-18,18-dimethyl-17-oxo-5,10-bis(pentafluorophenyl)porphyrin (Oxo-2). Treatment of a solution of **Oxo-Zn2** (7.5 mg, 10 μmol) in 0.4 mL of CH_2Cl_2 with 40 μL of TFA for 2 h followed by standard workup and chromatography [silica, hexanes/CH_2Cl_2 (3:2)] gave a reddish purple solid (5.6 mg, 82%): IR 1725 cm^{-1}; ^{1}H NMR δ −2.76 to −2.70 (br, 1H), −2.63 to −2.57 (br, 1H), 2.13 (s, 6H), 8.63 (d, J = 4.5 Hz, 1H), 8.68 (d, J = 4.5 Hz, 1H), 8.88−8.94 (m, 2H), 9.26−9.30 (m, 1H), 9.30−9.35 (m, 1H), 9.45 (s, 1H), 10.04 (s, 1H); LD-MS obsd 688.26; FAB-MS obsd 686.1151, calcd 686.1164 ($C_{34}H_{16}F_{10}N_4O$); λ_{abs} 413 (log ϵ = 5.08), 508 (3.99), 541 (3.71), 592 (3.60), 645 (4.30) nm; λ_{em} 645, 686, 715 nm.

17,18-Dihydro-18,18-dimethyl-5-(4-methylphenyl)-10-[4-[2-(trimethylsilyl)ethoxycarbonyl]phenyl]-17-oxoporphyrin (Oxo-3). Treatment of a solution of **Oxo-Zn3** (6.5 mg, 8.9 μmol) in 5 mL of CH_2Cl_2 with a 50-fold excess of TFA for 30 min followed by standard workup and chromatography [silica, hexanes/CH_2Cl_2 (1:3)] gave a purple solid (5.4 mg, 91%): ^{1}H NMR δ −2.46 to −2.42 (br, 1H), −2.31 to −2.27 (br, 1H), 0.17 (s, 9H), 1.26−1.32 (m, 2H), 2.11 (s, 6H), 2.70 (s, 3H), 4.59−4.63 (m, 2H), 7.55 (d, J = 8.0 Hz, 2H), 8.02 (d, J = 8.0 Hz, 2H), 8.23 (d, J = 8.0 Hz, 2H), 8.44 (d, J = 8.0 Hz, 2H), 8.56 (d, J = 4.8 Hz, 1H), 8.62 (d, J = 4.8 Hz, 1H),

8.84 (d, J = 4.8 Hz, 1H), 8.96 (d, J = 4.8 Hz, 1H), 9.10 (d, J = 4.8 Hz, 1H), 9.17 (d, J = 4.8 Hz, 1H), 9.25 (s, 1H), 9.86 (s, 1H); LD-MS obsd 663.06; FAB-MS obsd 665.2961, calcd 665.2948 ($C_{41}H_{40}N_4O_3Si$) $[M + H]^+$; λ_{abs} 416 (log ϵ = 5.28), 513 (4.10), 547 (3.92), 593 (3.79), 643 (4.25) nm; λ_{em} 643, 686, 713 nm.

5-(3,5-Di-*tert*-butylphenyl)-10-(4-ethynylphenyl)-17,18-dihydro-18,18-dimethyl-17-oxoporphyrin (Oxo-4). Treatment of a solution of **Oxo-Zn4** (9.8 mg, 14 μmol) in 5 mL of CH_2Cl_2 with a 50-fold excess of TFA for 1 h followed by standard workup and chromatography [silica, hexanes/CH_2Cl_2 (1:1)] gave a reddish purple solid (7.5 mg, 86%): ^{1}H NMR δ −2.40 to −2.36 (br, 1H), −2.27 to −2.24 (br, 1H), 1.52 (s, 18H), 2.11 (s, 6H), 3.32 (s, 1H), 7.80 (t, J = 1.6 Hz, 1H), 7.88 (d, J = 8.0 Hz, 2H), 7.99 (d, J = 1.6 Hz, 2H), 8.13 (d, J = 8.0 Hz, 2H), 8.60 (d, J = 4.4 Hz, 1H), 8.63 (d, J = 4.4 Hz, 1H), 8.87 (d, J = 4.4 Hz, 1H), 8.97 (d, J = 4.4 Hz, 1H), 9.10 (d, J = 4.4 Hz, 1H), 9.17 (d, J = 4.4 Hz, 1H), 9.23 (s, 1H), 9.85 (s, 1H); LD-MS obsd 641.80; FAB-MS obsd 643.3448, calcd 643.3437 ($C_{44}H_{42}N_4O$) $[M + H]^+$; λ_{abs} 417 (log ϵ = 5.30), 514 (4.10), 550 (3.92), 593 (3.77), 643 (4.25) nm; λ_{em} 643, 686, 713 nm.

5-(3,5-Di-*tert*-butylphenyl)-17,18-dihydro-10-(4-iodophenyl)-18,18-dimethyl-17-oxoporphyrin (Oxo-5). Treatment of a solution of **Oxo-Zn5** (10.2 mg, 12.6 μmol) in 5 mL of CH_2Cl_2 with a 50-fold excess of TFA for 1 h followed by standard workup and chromatography [silica, hexanes/CH_2Cl_2 (2:1)] gave a reddish purple solid (8.4 mg, 90%): ^{1}H NMR δ −2.42 to −2.38 (br, 1H), −2.29 to −2.25 (br, 1H), 1.52 (s, 18H), 2.10 (s, 6H), 7.80 (s, 1H), 7.90 (d, J = 7.6 Hz, 2H), 7.99 (s, 2H), 8.09 (d, J = 7.6 Hz, 2H), 8.60 (d, J = 4.4 Hz, 1H), 8.63 (d, J = 4.4 Hz, 1H), 8.87 (d, J = 4.4 Hz, 1H), 8.97 (d, J = 4.4 Hz, 1H), 9.10 (d, J = 4.4 Hz, 1H), 9.17 (d, J = 4.4 Hz, 1H), 9.24 (s, 1H), 9.85 (s, 1H); LD-MS obsd 742.81; FAB-MS obsd 745.2429, calcd 745.2403 ($C_{42}H_{41}IN_4O$) $[M + H]^+$; λ_{abs} 416 (log ϵ = 5.29), 513 (4.11), 547 (3.92), 589 (3.79), 643 (4.26) nm; λ_{em} 643, 687, 714 nm.

Cu(II)-17,18-dihydro-10-mesityl-18,18-dimethyl-5-(4-methylphenyl)porphyrin (Cu1). A solution of **1** (20 mg, 36 μmol) in 18 mL of CH_2Cl_2 was treated with a solution of Cu(OAc)$_2$·H$_2$O (160 mg, 800 μmol) in 2 mL of methanol at room temperature. The mixture was stirred overnight. Standard workup and chromatography [silica, CH_2Cl_2/hexanes (2:3)] gave a blue solid (19 mg, 85%): LD-MS obsd 608.43; FAB-MS obsd 609.2103, calcd 609.2079 ($C_{38}H_{34}CuN_4$); λ_{abs} 408 (log ϵ = 5.21), 501 (3.70), 569 (3.81), 605 (4.43) nm.

Cu(II)-17,18-dihydro-18,18-dimethyl-5,10-bis(pentafluorophenyl)porphyrin (Cu2). A solution of **2** (4.1 mg, 6.1 μmol) in 2 mL of CH_2Cl_2 was treated with a solution of Cu(OAc)$_2$·H$_2$O (100 mg, 500 μmol) in 0.5 mL of methanol at room temperature for 36 h. Standard workup and chromatography [silica, CH_2Cl_2/hexanes (2:3)] gave a blue solid (3.8 mg, 87%): LD-MS obsd 733.07; FAB-MS obsd 733.0533, calcd 733.0511 ($C_{34}H_{16}CuF_{10}N_4$); λ_{abs} 410 (log ϵ = 5.23), 505 (3.60), 568 (3.78), 611 (4.54) nm.

Cu(II)-5-(3,5-di-*tert*-butylphenyl)-10-(4-ethynylphenyl)-17,18-dihydro-18,18-dimethylporphyrin (Cu4). A solution of **4** (17.0 mg, 27.0 μmol) in 4 mL of CH_2Cl_2/methanol (1:1) was treated with Cu(OAc)$_2$·H$_2$O (135 mg, 0.675 mmol) at room temperature for 1.5 h. Standard workup and chromatography [silica, hexanes/CH_2Cl_2 (1:1)] gave a blue solid (16.0 mg, 86%): LD-MS obsd 688.68; FAB-MS obsd 689.2736, calcd 689.2705 ($C_{44}H_{42}CuN_4$); λ_{abs} (log ϵ = 5.31), 500 (3.75), 604 (4.55) nm.

Cu(II)-5-(3,5-di-*tert*-butylphenyl)-17,18-dihydro-10-(4-iodophenyl)-18,18-dimethylporphyrin (Cu5). A solution of **5** (14.5 mg, 19.8 μmol) in 4 mL of CH_2Cl_2/methanol (1:1) was treated with Cu(OAc)$_2$·H$_2$O (98.8 mg, 0.495 mmol) at room temperature for 2 h. Standard workup and chromatography [silica, hexanes/CH_2Cl_2 (1:1)] gave a blue solid (13.4 mg, 85%): LD-MS obsd 790.57; FAB-MS obsd 791.1719, calcd 791.1672 ($C_{42}H_{41}CuIN_4$); λ_{abs} 409 (log ϵ = 5.37), 510 (3.76), 604 (4.60) nm.

Cu(II)-17,18-dihydro-10-mesityl-18,18-dimethyl-5-(4-methylphenyl)-17-oxoporphyrin (Oxo-Cu1). A solution of **Oxo-1** (3.4 mg, 6.1 μmol) in 2.5 mL of CH_2Cl_2 was treated with a solution of Cu(OAc)$_2$·H$_2$O (120 mg, 600 μmol) in 0.5 mL of methanol. The mixture was stirred at room temperature for 36 h followed by 35 °C for 6 h. Standard workup and chromatography (silica, CH_2Cl_2) gave a blue solid (3.1 mg, 82%): IR 1719 cm^{-1}; LD-MS obsd 623.00; FAB-MS obsd 623.1861, calcd 623.1872 ($C_{38}H_{32}CuN_4O$); λ_{abs} 419 (log ϵ = 5.24), 605 (4.43) nm.

Cu(II)-17,18-dihydro-18,18-dimethyl-17-oxo-5,10-bis(pentafluorophenyl)porphyrin (Oxo-Cu2). A solution of **Oxo-2** (2.9 mg, 4.2 μmol) in 2.5 mL of CH_2Cl_2 was treated with a solution of Cu(OAc)$_2$·H$_2$O (100 mg, 500 μmol) in 0.5 mL of methanol. The mixture was stirred at room temperature for 48 h followed by 35 °C for 6 h. Standard workup and chromatography (silica, CH_2Cl_2) gave a blue solid (2.3 mg, 73%): LD-MS obsd 744.33; FAB-MS obsd 747.0341, calcd 747.0304 ($C_{34}H_{14}CuN_4O$); λ_{abs} 418 (log ϵ = 5.27), 610 (4.51) nm.

Cu(II)-5-(3,5-di-*tert*-butylphenyl)-10-(4-ethynylphenyl)-17,18-dihydro-18,18-dimethyl-17-oxoporphyrin (Oxo-Cu4). A solution of **Oxo-4** (14.8 mg, 23.0 μmol) in 5 mL of CH_2Cl_2/methanol (1:1) was treated with Cu(OAc)$_2$·H$_2$O (115 mg, 0.575 mmol) at room temperature for 2 h. Standard workup and chromatography [silica, hexanes/CH_2Cl_2 (1:1)] gave a blue solid (15.3 mg, 94%): LD-MS obsd 702.78; FAB-MS obsd 703.2512, calcd 703.2498 ($C_{44}H_{40}CuN_4O$); λ_{abs} 420 (log ϵ = 5.41), 560 (3.88), 605 (4.55) nm.

Cu(II)-5-(3,5-di-*tert*-butylphenyl)-17,18-dihydro-10-(4-iodophenyl)-18,18-dimethyl-17-oxoporphyrin (Oxo-Cu5). A solution of **Oxo-5** (17.2 mg, 23.1 μmol) in 5 mL of CH_2Cl_2/methanol (1:1) was treated with Cu(OAc)$_2$·H$_2$O (115 mg, 0.575 mmol) at room temperature for 2 h. Standard workup and chromatography [silica, hexanes/CH_2Cl_2 (1:1)] gave a blue solid (16.8 mg, 90%): LD-MS obsd 805.45; FAB-MS obsd 805.1486, calcd 805.1465 ($C_{42}H_{39}CuIN_4O$); λ_{abs} 420 (log ϵ = 5.41), 560 (3.88), 605 (4.55) nm.

Mg(II)-17,18-dihydro-10-mesityl-18,18-dimethyl-5-(4-methylphenyl)porphyrin (Mg1). Following a standard procedure,[39] a mixture of **1** (5.0 mg, 9.1 μmol), MgI_2 (25 mg, 89 μmol), and *N*,*N*-diisopropylethylamine (31 μL, 180 μmol) in 0.5 mL of CH_2Cl_2 was stirred for 3 h at room temperature. The fluorescence excitation spectrum of an aliquot taken at this stage indicated total consumption of **1**. The mixture was treated with 10% aqueous $NaHCO_3$. The organic layer was separated, dried (Na_2SO_4), and concentrated. The title compound underwent demetalation during workup. A peak corresponding to M^+ was not visible in the LD-MS spectrum.

Mg(II)-17,18-dihydro-10-mesityl-18,18-dimethyl-5-(4-methylphenyl)-17-oxoporphyrin (Oxo-Mg1). Following a standard procedure,[39] a mixture of **Oxo-1** (5.0 mg, 8.9 μmol), MgI_2 (25 mg, 89 μmol), and *N*,*N*-diisopropylethylamine (31 μL, 180 μmol) in 0.5 mL of CH_2Cl_2 was stirred for 3 h. Standard workup and chromatography [basic alumina, grade V, CH_2Cl_2/methanol (199:1)] gave a green solid (2.0 mg, 38%): IR 1717 (weak), 1675 (strong) cm^{-1}; ^{1}H NMR δ (THF-d_8) 1.84 (s, 6H), 2.00 (s, 6H), 2.58 (s, 3H), 2.65 (s, 3H), 7.24 (s, 2H), 7.49 (d, J = 8.4 Hz, 2H), 7.95 (d, J = 8.4 Hz, 2H), 8.30 (d, J = 4.4 Hz, 1H), 8.39 (d, J = 4.4 Hz, 1H), 8.44 (d, J = 4.4 Hz, 1H), 8.61 (d, J = 4.4 Hz, 1H), 8.78 (d, J = 4.4 Hz, 1H), 8.81 (d, J = 4.4 Hz, 1H), 8.87 (s, 1H), 9.38 (s, 1H); MALDI-MS obsd 583.77; FAB-MS obsd 584.2445, calcd 584.2427 ($C_{38}H_{32}N_4OMg$); λ_{abs} 425 (log ϵ = 5.28), 568 (3.92), 617 (4.54) nm; λ_{em} 617, 659, 672 nm.

Mg(II)-17,18-dihydro-18,18-dimethyl-17-oxo-5,10-bis(pentafluorophenyl)porphyrin (Oxo-Mg2). Following a standard procedure,[39] a mixture of **Oxo-2** (7.80 mg, 11.4 μmol), MgI_2 (31.7 mg, 114 μmol), and *N*,*N*-diisopropylethylamine (40 μL, 230 μmol) in 1 mL of CH_2Cl_2 was stirred for 2 h. Additional MgI_2 (31.7 mg, 114 μmol) and *N*,*N*-diisopropylethylamine (40

μL, 230 μmol) were added, and then the mixture was stirred for 2 h. Standard workup and chromatography [basic alumina, grade V, CH_2Cl_2 then CH_2Cl_2/methanol (199:1)] gave a purple solid (6.8 mg, 84%): ^{1}H NMR δ (THF-d_8) 2.07 (s, 6H), 8.64 (d, J = 4.4 Hz, 1H), 8.69 (d, J = 4.4 Hz, 1H), 8.75−8.81 (m, 2H), 9.05 (d, J = 4.4 Hz, 1H), 9.90 (d, J = 4.4 Hz, 1H), 9.23 (s, 1H), 9.69 (s, 1H); MALDI-MS obsd 707.50; FAB-MS obsd 708.0887, calcd 708.0858 ($C_{34}H_{14}F_{10}MgN_4O$); λ_{abs} 425, 537, 620 nm; λ_{em} 621, 663, 680 nm.

B. Physical Methods. 1. Static Absorption and Emission Spectroscopy. Static absorption (HP-8453 or Cary 100) and fluorescence (Spex Fluoromax or Tau2) measurements were performed as described previously.[62] For emission studies, nondeaerated samples with an absorbance ≤0.15 at λ_{exc} (typically 0.3−0.8 μM) were employed, with λ_{exc} in either the Soret or Q-band region; the detection band-pass was 2−5 nm, and the spectra were corrected for the detection-system spectral response. Emission quantum yields were measured relative to the reference compounds **FbTPP** (Φ_f = 0.11)[42] or **ZnTPP** (Φ_f = 0.033).[40]

2. Time-Resolved Fluorescence Spectroscopy. Fluorescence lifetimes were obtained on samples that had concentrations of 0.5−10 μM and were deaerated by bubbling with N_2. Lifetimes were determined by fluorescence modulation (phase shift) techniques using a Spex Tau2 spectrofluorimeter. Samples were excited at various wavelengths and detected through appropriate colored glass filters. Modulation frequencies from 20 to 300 MHz were utilized, and both the fluorescence phase shift and modulation amplitude were analyzed.

3. Time-Resolved Absorption Spectroscopy. Transient absorption data were acquired as described previously.[62] Samples (∼10 μM in toluene) in 2 mm path length cuvettes at room temperature were excited at 10 Hz with ∼130 fs, 5−30 μJ pulses at the appropriate wavelength and probed with white-light probe pulses of comparable duration.

4. Resonance Raman Spectroscopy. The resonance Raman spectra were recorded using the same instrumentation (spectrometer, lasers, etc.) as previously described.[63] The samples typically had a concentration of 100 μM (in CH_2Cl_2) and were contained in 1 mm i.d. capillary tubes. The laser power at the sample was typically 10 mW, and the spectral resolution was ∼3 cm^{-1} at a Raman shift of 1600 cm^{-1}.

5. Electrochemistry. The electrochemical measurements were performed using instrumentation and methods previously described.[43] The solvent was CH_2Cl_2 containing 0.1 M Bu_4NPF_6.

Acknowledgment. This research was supported by grants from the NIH (GM36238) (to J.S.L.) and the NSF (CHE-9988142). Mass spectra were obtained at the Mass Spectrometry Laboratory for Biotechnology. Partial funding for the Facility was obtained from the North Carolina Biotechnology Center and the National Science Foundation. S.P. thanks Cochin University of Science and Technology for a sabbatical leave.

Supporting Information Available: Complete spectral data (absorption, fluorescence, ^{1}H NMR, LD-MS) for all new chlorins and oxochlorins. This material is available free of charge via the Internet at http://pubs.acs.org.

JO025843I

(62) (a) Yang, S. I.; Li, J.; Cho, H. S.; Kim, D.; Bocian, D. F.; Holten, D.; Lindsey, J. S. *J. Mater. Chem.* **2000**, *10*, 283−296. (b) Yang, S. I.; Lammi, R. K.; Seth, J.; Riggs, J. A.; Arai, T.; Kim, D.; Bocian, D. F.; Holten, D.; Lindsey, J. S. *J. Phys. Chem. B* **1998**, *102*, 9426−9436.

(63) Zhou, C.; Diers, J. R.; Bocian, D. F. *J. Phys. Chem. B* **1997**, *101*, 9635−9644.